

Thermal Diffusion in Liquids*

by

Jeong-long Lin

Department of Chemistry
Boston College
Chestnut Hill, MA 02167

Thermal Diffusion in Gases

by

William L. Taylor

EG&G Mound Applied Technologies, Inc.,[†]
Miamisburg, OH 45343
and
Department of Chemistry
University of Cincinnati
Cincinnati, OH 45221

This document is
PUBLICLY RELEASABLE



Authorizing Official
Date: 6-17-89

* This research is supported by the National Science Foundation (CHE-8719039)

[†] EG&G Mound Applied Technologies is operated for the U.S. Department of Energy under Contract No. DE-AC04-88DP43495

TABLE OF CONTENTS

General	1
Thermal Diffusion in Liquids	8
Frames of Reference	8
Experimental Methods	11
The Soret Effect	12
(a) The potentiometric Method	13
(b) The conductimetric Method	18
(c) The Flow-Cell Method	21
(d) The Optical Method	23
The Dufour Effect (The Diffusion Thermoeffect)	24
Experimental Data and Discussion	28
Thermal Diffusion in Gases	36
The Two-Bulb Method	38
The Trennschaukel (Swing Separator)	44
The Thermal Diffusion Column	50
The Dufour Effect	55
Symbol Table	59
References	63

1.0 General

In a mixture in either the condensed or gaseous phase in which the temperature is steady but not uniform, transport of both matter and heat may be observed. The process is known as thermal diffusion, and in condensed phases it is also known as the Soret effect, a direct measure of the degree of separation being the Soret coefficient σ [1]. In the gas phase the degree of separation is known as the thermal diffusion factor α_T . The separation is a molecular migration of the components due to a temperature gradient. The inverse phenomenon, the development of a temperature gradient due to diffusion, is called the Dufour effect [2]. The transport of matter and heat are generally coupled. When the driving forces of thermal diffusion, the gradients of temperature and chemical potential, are sufficiently small, and the observed heat and matter fluxes are linear in the forces, thermal diffusion in either the condensed or gaseous phase may be described in terms of non-equilibrium thermodynamics, and the inverse effects related through the Onsager cross phenomenological coefficients for heat and matter flow [3 - 6].

The thermal diffusion phenomenon may be expressed in terms of a number of transport properties whose specific definitions in terms of experimental parameters are derived in the following through non-equilibrium thermodynamics. The typical ones are the previously mentioned measures of separation (σ and α_T), the coefficients of thermal (D^T) and ordinary (D_{12}) diffusion and the heat (Q^*) and entropy (S^*) of transport. The equivalence of the thermal diffusion and Dufour (D^D) coefficients is given by the Onsager reciprocal relations.

To derive these transport properties and their interactions we consider a system of n components in mechanical equilibrium at constant pressure and assume that the only processes occurring are those of heat and matter transport, which are linear processes. The derivation follows from the expression for the entropy flux and the entropy balance equation. In general there is an empirical relationship between a flow or flux, \vec{J} , and a driving force, \vec{X} , of the form

$$\vec{J} = \begin{vmatrix} L_{11} & \cdot & \cdot & \cdot & L_{1n} \\ \cdot & & & & \cdot \\ \cdot & & & & \cdot \\ \cdot & & & & \cdot \\ L_{n1} & \cdot & \cdot & \cdot & L_{nn} \end{vmatrix} \begin{pmatrix} \vec{X}_1 \\ \cdot \\ \cdot \\ \cdot \\ \vec{X}_n \end{pmatrix} \quad (1)$$

where the L_{ij} are scalar quantities similar to a conductance, reciprocal resistance or an affinity. The most general set of linear equations is

$$\vec{J}_i = \sum_j L_{ij} \vec{X}_j \quad (2)$$

where the L_{ij} are known as the phenomenological coefficients. The diagonal coefficients L_{ii} represent the direct effects, and the off-diagonal coefficients $L_{ij} (i \neq j)$ represent the coupled effects. The heat flux is designated \vec{J}_q , and the entropy change is dq divided by the absolute temperature. For heat and matter transport the entropy flux, \vec{J}_s , is

$$\vec{J}_s = \frac{1}{T} \left(\vec{J}_q - \sum_j \mu_j \vec{J}_j \right) \quad (3)$$

with the μ_j being the chemical potentials.

Conservation of entropy requires that the rate of change of entropy in a unit volume be equal to the flow out plus any internal source of production. Denoting S_v as the entropy of the fluid per unit volume, the local change equations for entropy, heat, and matter are

$$\frac{dS_v}{dt} = -\text{div } \vec{J}_s + \Phi \quad (4)$$

$$\frac{\partial q_v}{\partial t} = -\text{div } \vec{J}_q, \text{ and} \quad (5)$$

$$\frac{\partial c_j}{\partial t} = -\text{div } \vec{J}_j \quad (6)$$

In Equation (4) Φ is the source term for entropy production within the unit volume from irreversible processes and must be zero. The w_j in Equation (6) are the mass fractions of the components. Onsager has chosen the forces in such a way that the product of the internal entropy source and the absolute temperature is equal to the sum of the flows \vec{J}_j multiplied by the conjugate forces \vec{X}_j .

$$\begin{aligned} T\Phi &= \sum_k \vec{J}_k \cdot \vec{X}_k \\ &= \vec{J}_q \cdot \vec{X}_q + \sum_j \vec{J}_j \cdot \vec{X}_j \end{aligned} \quad (7)$$

The units of Equation (7) are $\text{Jm}^{-3}\text{s}^{-1}$. The dissipation function $T\Phi$ is invariant with respect to choice of forces and fluxes and may therefore be described by different sets of fluxes and their respective conjugate forces which are related through the Onsager phenomenological coefficients. In general a reduced heat flux can be defined as

$$\vec{J}_q = \vec{J}_q - \sum_j H_j \vec{J}_j \quad (8)$$

Substituting Equation (8) into Equation (7) produces

$$\begin{aligned} T\Phi &= \bar{X}_q \left(\bar{J}_q + \sum_j \bar{H}_j \bar{J}_j \right) + \sum_j \bar{J}_j \cdot \bar{X}_j \\ &= \bar{J}_q \cdot \bar{X}_q + \sum_j \bar{J}_j \cdot (\bar{H}_j \bar{X}_q + \bar{X}_j). \end{aligned} \quad (9)$$

In Equation (9) the partial molar enthalpy of the j^{th} component is \bar{H}_j . A suitable choice of forces corresponding to fluxes of heat and matter, respectively, is given by Equations (10) and (11):

$$\bar{X}_q = \text{grad}(1/T) \quad (10)$$

and

$$\bar{X}_j = \text{grad}(-\mu_j/T) \quad (11)$$

The heat and material flux equations then become, respectively,

$$\bar{J}_q = L_{qq} \text{grad}(1/T) + \sum_j L_{qj} \text{grad}(-\mu_j/T) \quad (12)$$

and

$$\bar{J}_i = L_{iq} \text{grad}(1/T) + \sum_j L_{ij} \text{grad}(-\mu_j/T). \quad (13)$$

The matrix of phenomenological coefficients is symmetric, i.e., $L_{ij} = L_{ji}$, according to the Onsager reciprocity relation. They are the generalized transport coefficients and are the subjects of experimental determination. To show this we define \bar{H}_j such that

$$L_{iq} = \sum_j L_{ij} \bar{H}_j = L_{qi} \quad (14)$$

and substitute Equation (14) into Equations (12) and (13) to yield

$$\bar{J}_q = \left(L_{qq} - \sum_i \sum_j L_{ij} \bar{H}_j \right) \text{grad}(1/T) + \sum_j \bar{H}_j \bar{J}_j \quad (15)$$

and

$$\vec{J}_i = \sum_j L_{ij} \left\{ \bar{H}_j \text{grad}(1/T) + \text{grad}(-\mu_j/T) \right\}. \quad (16)$$

Under isothermal conditions, i.e. the temperature gradient is zero, Equation (15) becomes

$$\vec{J}_q = \sum_j \bar{H}_j \vec{J}_j. \quad (17)$$

Equation (17) suggests that \bar{H}_j is the transported enthalpy of species j under isothermal conditions. The reduced heat of transport, Q_j^* , when $\text{grad } T = 0$, is

$$\vec{J}_q' = \sum_j \bar{H}_j \vec{J}_j - \sum_j H_j \vec{J}_j \quad (18)$$

so that

$$\sum_j Q_j^* \vec{J}_j = \sum_j \bar{H}_j \vec{J}_j - \sum_j H_j \vec{J}_j \quad (19)$$

or

$$Q_j^* = \bar{H}_j - H_j = -\frac{\text{grad } \mu_j}{\text{grad } \ln T}. \quad (20)$$

It then follows that

$$\vec{J}_q' = \sum_j Q_j^* \vec{J}_j. \quad (21)$$

The reduced (or "corrected") heat of transport, Q_j^* , is the enthalpy of transport less the partial enthalpy carried by species j , or in other words, the heat supplied to or absorbed by the thermostat to maintain the system in an isothermal condition. When all fluxes are independent, \bar{H}_j may be measured at the steady state (ss). Setting all $\vec{J}_i = 0$, Equation (16) yields

$$\bar{H}_j = \left[\text{grad}(\mu_j/T) / \text{grad}(1/T) \right]_{ss} = L_{iq} / L_{ij}. \quad (22)$$

This may not be obvious from Equation (16) unless this equation is expanded in matrix form:

$$\begin{pmatrix} \vec{J}_1 \\ \cdot \\ \cdot \\ \cdot \\ \vec{J}_n \end{pmatrix} = \begin{pmatrix} L_{11} & \cdot & \cdot & \cdot & L_{1n} \\ \cdot & & & & \cdot \\ \cdot & & & & \cdot \\ \cdot & & & & \cdot \\ L_{n1} & \cdot & \cdot & \cdot & L_{nn} \end{pmatrix} \begin{pmatrix} \vec{X}_1 + \bar{H}_1 \vec{X}_q \\ \cdot \\ \cdot \\ \cdot \\ \vec{X}_n + \bar{H}_n \vec{X}_q \end{pmatrix} \quad (23)$$

The first expansion term is

$$\vec{J}_1 = L_{11} (\vec{X}_1 + \bar{H}_1 \vec{X}_q) + L_{12} (\vec{X}_2 + \bar{H}_2 \vec{X}_q) + \dots \quad (24)$$

from which it follows that all \vec{J}_i must be set equal to zero in order for each term $(\vec{X}_j + \bar{H}_j \vec{X}_q)$ to be equal to zero. Equivalently, if every element of the l.h.s. matrix is zero, every element of the $(\vec{X}_j + \bar{H}_j \vec{X}_q)$ column vector must also be zero, since the L-matrix has no zero elements.

The above analysis may also be carried out in terms of the entropy fluxes \vec{J}_s and \vec{J}_s' . Denoting $\bar{\vec{S}}_j$ as the transported entropy, $\bar{\vec{S}}_j = \bar{S}_j + S_j^*$, one obtains:

$$\vec{J}_s = \sum_j \bar{\vec{S}}_j \vec{J}_j \quad (25)$$

$$\vec{J}_s' = \sum_j S_j^* \vec{J}_j - \sum_j \bar{S}_j \vec{J}_j \quad (26)$$

At the limiting isothermal state S_j^* may be measured at the steady state and is given by

$$T S_j^* = [\text{grad } \mu_j / \text{grad } (-\ln T)]_{ss} \quad (27)$$

From the Gibb's free energy, $G = H - TS$, and the definition of the chemical potential at constant temperature and pressure, $\mu_j = (\partial G / \partial n_j)_{T,p,n}$, one arrives at

$$\bar{H}_j = T \bar{S}_j + \mu_j \quad (28)$$

Combining Equations (20) and (27) leads to

$$T S_j^* = Q_j^* . \quad (29)$$

The implication of Equations (28) and (29) is interesting. Particles taking part in linear transport processes carry with them a non-zero heat (enthalpy) and entropy of transport. However the chemical potential of transport, i.e. for a moving j , is zero. This follows because of the principle of local equilibrium [7].

The heat and entropy of transport must obey a conservation relation. This may be deduced from Equation (27) which requires at the steady state that

$$- \text{grad } \mu_j = \bar{S}_j \text{ grad } T . \quad (30)$$

Multiplying the above equation by $\sum_j x_j$ yields

$$- \sum_j x_j \text{ grad } \mu_j - \sum_j x_j \bar{S}_j \text{ grad } T = \sum_j x_j S_j^* . \quad (31)$$

where the x_j are the mole fractions.

Now the Gibbs-Duhem equation can be used to define partial molar quantities in terms of any extensive state function. In terms of the chemical potential and partial molar entropies at constant pressure

$$\left(\partial \mu_j / \partial T \right) = - \bar{S}_j \quad (32)$$

and Equation (31) reduces to

$$\sum_j x_j S_j^* = 0 . \quad (33)$$

It should also be noted that S_j^* and Q_j^* are independent of the frame of reference of the diffusion fluxes. This is because the dissipation function is invariant with respect to the frame of reference.

For a binary system the phenomenological coefficients appearing in the flux equations can be defined in a slightly different form which defines the macroscopic quantities to be measured

by the experiments discussed later. These quantities are the thermal diffusion (or Soret), Dufour, mass diffusion, and thermal conductivity coefficients. They are, respectively:

$$D^T = L_{iq} \bar{M} / (\rho x_1 x_2 T^2) \quad (34)$$

$$D^D = L_{qi} \bar{M} / (\rho x_1 x_2 T^2) \quad (35)$$

$$D_{12} = L_{11} \bar{M} \left(\frac{\partial \mu_1}{\partial x_1} \right)_{P, T, x_2} / (\rho x_2 T) \quad (36)$$

$$\kappa = L_{qq} / T^2 \quad (37)$$

where $\bar{M} = x_1 M_1 + x_2 M_2$ and the M_i are the molecular weights.

From the equivalence of L_{iq} and L_{qi} , it follows that $D^T = D^D$; the existence of a thermal gradient gives rise to a concentration gradient and vice versa.

1.1 Thermal Diffusion in Liquids

Thermal diffusion is a well recognized tool for the study of molecular interactions in the gas phase. The phenomenon is strongly influenced by the form of the intermolecular potential energy relationship, and data derived from thermal diffusion experiments with gas phase mixtures provide a sensitive test of proposed models for the potential energy function.

Thermal diffusion in liquids, or the Soret effect [1], can also yield useful information about liquid phase systems. In recent years the study of the Soret effect has taken on a new significance and has yielded new and interesting information about the nature of solutions. Thermal diffusion data are expected to be useful in the investigation of the nature of interaction in solutions and perhaps especially in those areas where dynamics and the structure are involved. Soret data, for example, have been found to be particularly helpful in understanding ionic hydration structure in electrolyte solutions [8].

The Soret effect in liquids can be investigated through the measurements of a number of transport properties. The typical ones are the thermal diffusion coefficient D_T , the Soret coefficient σ , and the heat Q^* and entropy S^* of transport. In preparation for the discussion of experimental techniques it is worthwhile to consider the effect of the frame of reference on these quantities.

1.1.1 Frames of Reference

S_i^* and Q_i^* are independent of the frame of reference of the diffusion fluxes. This is because the dissipation function is an invariant with respect to the frame of reference. To show this we transform fluxes \vec{J}_i to fluxes \vec{J}_i^F in the frame F . Denoting \vec{u}^F as the velocity of the new frame, \vec{J}_i^F is given by

$$\vec{J}_i^F = \vec{J}_i - c_i \vec{u}^F \quad (38)$$

The dissipation function in terms of \vec{J}_i^F is

$$\begin{aligned} T\Phi &= \vec{J}_q \cdot \text{grad}(-\ln T) + \sum \vec{J}_i \cdot \text{grad}_T(-\mu_i) \\ &= \vec{J}_q \cdot \text{grad}(-\ln T) + \sum \vec{J}_i^F \cdot \text{grad}_T(-\mu_i) + \vec{u}^F \cdot \sum c_i \text{grad}_T(-\mu_i) \\ &= \vec{J}_q \cdot \text{grad}(-\ln T) + \sum \vec{J}_i^F \cdot \text{grad}_T(-\mu_i) \end{aligned} \quad (39)$$

Thus, by defining Q_i^{*F} as the heat of transport associated with the fluxes \vec{J}_i^F , it can be shown that,

$$\begin{aligned} \vec{J}_q &= \sum \vec{J}_i Q_i^* = \sum \vec{J}_i^F Q_i^{*F} \\ &= \sum \vec{J}_i^F Q_i^* + \vec{u}^F \sum c_i Q_i^* = \sum \vec{J}_i^F Q_i^* \end{aligned} \quad (40)$$

by noting that $\sum c_i Q_i^* = 0$. It follows from Equation (40) that, $Q_i^{*F} = Q_i^*$, provided that the fluxes \vec{J}_i^F are all independent.

Although the heat of transport is independent of the frame of reference, diffusion fluxes in different frames may not give rise to the same experimental heat of transport. Three frequently adopted fluxes are; the mass \vec{J}_i^m , volume \vec{J}_i^V and Hittorf \vec{J}_i^H frames of reference. The fluxes in each frame are mutually dependent and the relationship can be expressed by the equation

$$\sum r_i^F \vec{J}_i^F = 0 \quad (41)$$

where $r_i^m = 1$, $r_i^V = \bar{V}_i$, the partial molar volume of i and $r_i^H = \delta_{i0}$. By substituting Equation (41) into Equation (40), one obtains

$$\begin{aligned} \vec{J}_q &= \sum \vec{J}_i^F Q_i^* = \sum_{i \neq 0} \vec{J}_i^H Q_i^* \\ &= \sum_{i \neq r} \vec{J}_i^m (Q_i^* - Q_r^*) = \sum_{i \neq r} \vec{J}_i^V (Q_i^* - Q_r^* \bar{V}_i / \bar{V}_r) \end{aligned} \quad (42)$$

where r indicates the reference component chosen.

Equation (42) implies that for two component ($i = 0$ and 1) mixtures, when the \vec{J}_i^H is adopted, the heat of transport that is measured is Q_1^* . On the other hand if \vec{J}_i^m or \vec{J}_i^V is used, the relative heat of transport, $(Q_1^* - Q_0^*)$ or $(Q_1^* - Q_0^* \bar{V}_1 / \bar{V}_0)$ is obtained. Since the differences are a likely source of error when comparing thermal diffusion data among different experiments, it is useful to ascertain the uncertainties. For a binary mixture and from Equation (33),

$$Q_1^* - Q_0^* = Q_1^* + c_1 Q_0^* / c_0 = Q_1^* (c_0 + c_1) / c_0 \quad (43)$$

Thus $Q_i^* - Q_o^*$ measured with \vec{J}_i^m differs from Q_i^* measured with \vec{J}_i^H by a factor, $(c_o + c_i) / c_o$. For dilute solutions this factor approaches unity and the results in two experiments are identical. This same analysis can be applied to experiments based on the volume-fixed frame of reference.

In electrolyte solutions ionic fluxes are mutually dependent because of the electroneutrality requirement. For a simple electrolyte solution containing solvent (O), and one species each of the cation (+) and anion (-), the electroneutrality condition $v_+ Z_+ + v_- Z_- = 0$ requires that

$$\vec{J}_{\text{salt}} = \vec{J}_+ / v_+ = \vec{J}_- / v_- \quad (44)$$

Here Z_i is the ionic valence, and v_i measures the number of moles of ion i produced from one mole of the salt. The expression for the reduced heat flux is

$$\begin{aligned} \vec{J}_q' &= \vec{J}_o Q_o^* + \vec{J}_{\text{salt}} (v_+ Q_+^* + v_- Q_-^*) \\ &= \vec{J}_o Q_o^* + \vec{J}_{\text{salt}} Q_{\text{salt}}^* \end{aligned} \quad (45)$$

Equation (45) shows that a simple electrolyte solution is a binary system, and only the molar heat of transport, $Q_{\text{salt}}^* = v_+ Q_+^* + v_- Q_-^*$, can be measured experimentally using J_{salt}^H . It is Q_{salt}^* and not Q_{ion}^* that is independent of the frame of reference in a simple electrolyte solution.

Other thermal diffusion properties such as the thermal diffusion coefficients and the Soret coefficients can also be expressed in terms of the fluxes. A convenient frame of reference for this discussion is the Hittorf frame of reference. For a binary solution the phenomenological equations are,

$$\vec{J}_q' = L_{qq} \text{grad} (-\ln T) + L_{q1} \text{grad}_T (-\mu_1) \quad (46)$$

$$\vec{J}_1^H = L_{1q} \text{grad} (-\ln T) + L_{11} \text{grad}_T (-\mu_1) \quad (47)$$

where in the case of a simple electrolyte solution denoting $\tilde{\mu}_i$ as the electrochemical potential of the ion i ,

$$\mu_1 = \mu_{\text{salt}} = v_+ \mu_+ + v_- \mu_- = v_+ \tilde{\mu}_+ + v_- \tilde{\mu}_- \quad (48)$$

The isothermal diffusion coefficient D_1 and the thermal diffusion coefficient D_1^T are defined in terms of \vec{j}_1^H as

$$\vec{j}_1^H = -D_1 \text{grad}c_1 - c_1 D_1^T \text{grad}T \quad (49)$$

Comparing Equations (48) and (49), one arrives at the results,

$$D_1 = L_{11} \left(\frac{\partial \mu_1}{\partial c_1} \right)_{T,P} / T \quad \text{and} \quad D_1^T = L_{1q} / T^2 c_1 \quad (50)$$

D_1 is commonly defined in terms the molarity c_1 . However, the Soret coefficient and heat of transport are more conveniently defined in terms of the molality m_1 . Thus, to relate D_1 and D_1^T to σ_1 and Q_1^* , a conversion factor, $f = (\partial m_1 / \partial c_1)$ is required [9]. In cases where solutions are very dilute, $f \rightarrow 1$ and one obtains

$$\sigma = D_1^T / D_1 = Q_1^* / \left(\frac{\partial \mu_1}{\partial \ln m_1} \right)_{PT} / T \quad (51)$$

It should be pointed out also that in Equation (49) the isothermal diffusion coefficient is defined in the Hittorf (solvent-fixed) frame, which is not the same as the experimental diffusion coefficient measured in the volume frame of reference. Transformations exist, however, for passing from one frame to another. Although both solvent-fixed and volume-fixed diffusion coefficients are identical at infinite dilution, they diverge significantly in concentrated solution [10].

1.1.2 Experimental Methods

Methods of studying the Soret effect and the calculation of the Soret coefficient and other thermal diffusion properties in liquids up to 1961 have been summarized in a monograph by Tyrrell [11]. Our task here will, therefore, be devoted to providing a brief account of more recent work in this field. The investigation, in liquids, of the Dufour effect (the heat flow associated with a concentration gradient) is relatively new. This is perhaps because of the relatively high thermal conductivities of liquids, which makes experimental measurements difficult. (In contrast, both theory and experiment for the study of the Dufour effect in gases have been well developed).

1.1.2.1. The Soret Effect

In the study of the Soret effect most measurements start by applying a constant temperature gradient to an isothermal homogeneous solution. As the concentration of the solution becomes non-uniform due to thermal diffusion, an opposing process of ordinary diffusion develops which eventually exactly balances the thermal diffusion process, thereby leading the system to a Soret steady-state. The Soret coefficient and the heat of transport are then derived from the steady-state concentration gradient. Although it is the steady-state property that we measure, the approach to the steady-state needs to be followed in order to verify the phenomenology of the thermal diffusion process.

In a typical pure thermal diffusion experiment, the solution is placed in a flat cell and a one-dimensional temperature gradient (usually of the order less than $10^{\circ} \text{ cm}^{-1}$ and in the direction opposite to the gravitational field) is applied by bringing the flat end-plates of the cell into contact with heat reservoirs maintained at temperature T' and T'' . For a binary solution the rate of change of concentration during the establishment of the Soret steady-state can be written as [12],

$$\begin{aligned} \Delta m_t &= \Delta m_{st} [1 - g(t)] \\ &= \Delta m_{st} \left\{ 1 - \left(8/\pi^2 \right) \sum \left(1/n^2 \right) \exp \left[-n^2 (t-t')/\theta \right] \right\} \quad (52) \\ n &= 1, 3, \dots \end{aligned}$$

where $\Delta m_t = m'' - m'$ at time t (measured from the instant the temperature gradient is applied) and m'' and m' are the molalities at temperatures T'' and T' , respectively. The thermal diffusion relaxation time is $\theta = a^2/\pi^2 D$ where a is the distance between the end-plates, and D is the effective diffusion coefficient. When $|T'' - T'|$ is small, D is, to a good approximation, the isothermal diffusion coefficient at the mean temperature $T = 1/2 (T' + T'')$. The warming-up correction is accounted for by t' . Assuming that the end-plates warm up exponentially with a characteristic time τ ,

$$t' = \tau - (a^2/12K) \quad (53)$$

where K is the thermal diffusivity of the liquid. When K is infinitely large the end-plates warm up instantaneously, resulting in $\tau = 0$ and $t' = 0$.

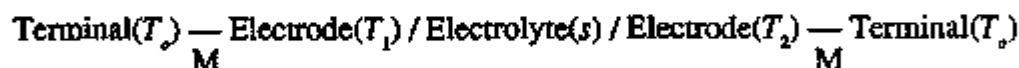
Equation (53) is due to Agar [13]. The warming-up correction t' can be positive or negative in sign, and there is a plausible qualitative rationale. During the warming-up period the temperature gradient (and hence the local rate of thermal diffusion) exceeds that of the steady-state value near the end of the cell, but lags behind in the central regions; the net balance of these effects in time and space, while the thermal transients decay, governs the sense of the correction. When $t' < 0$, the warming-up correction acts in the gained-time sense. The warming-up correction has also been discussed by Horne and Anderson [14]. Their analysis results in requiring that the warming-up correction always act in the lost-time sense. This seems an unrealistic prediction. A discussion of this can be found in Lin, Bierlein and Becsey [15].

Equation (52) gives rise to the changes in other solution properties such as the thermal e.m.f., conductance, the refractive index, etc. Thus the Soret effect can be investigated by the potentiometric, conductimetric and optical methods. There are also methods based on direct measurement of the concentration gradient at the steady state. One example of the latter is the flow cell method.

Thermal diffusion properties have also often been investigated using the thermogravitational column. We shall, however, not discuss the latter method since the separation is facilitated by the convection, and the method is not a direct method designed for the study of the pure Soret effect.

(a) The Potentiometric Method. [16]

This method is limited to electrolyte systems for which stable electrodes can be found. The electrolyte is confined in a cell (thermocell) which has electrically insulating sidewalls between end-plates, which also serve as electrodes. The simplest thermocell employs two identical electrodes kept at different temperatures, such as;



The sign convention is such that a positive thermal e.m.f. E of the thermocell causes the current to flow from hot to cold in metallic conductor(s) M . Consider the thermocell with electrode reaction

$$\sum \lambda_j A_j + \sum \lambda_r A_r + e = 0 \quad (54)$$

in which ionic and molecular constituents of the solution are denoted by A_j , and possible substances existing in phases other than the solution by A_r . The stoichiometric coefficient is taken as zero for those substances that do not take part in the electrode reaction. The thermal e.m.f.

dE_t at time t after a temperature difference of dT has been applied to the two electrodes is given by [16,17]

$$F dE_t = F dE_{st} + \sum (\lambda_j - W_j) \left(\frac{\partial \mu_j}{\partial m_j} \right)_{P,T} dm_{j,t} + \sum (\lambda_j - W_j) S_j^* dT \quad (55)$$

where F is the Faraday constant, W_j is the Washburn number (the transport number t_j divided by the ionic valence) and $dm_{j,t}$ denotes the concentration difference of the species j at the surfaces of the electrodes at time t . Note that at time $t = 0$, that is the instant when the temperature gradient is applied, the solution is homogeneous. Thus, $dm_{j,t} = 0$ and

$$F (dE_{st} - dE_o) = \sum (W_j - \lambda_j) S_j^* dT \quad (56)$$

or

$$F (\epsilon_{st} - \epsilon_o) = \sum (W_j - \lambda_j) S_j^* \quad (57)$$

where $\epsilon = dE/dT$ is the thermoelectric power. For a simple electrolyte solution, assuming that the electrode is reversible to ion 1 of the two ionic species $\lambda_1 = Z_1^{-1}$, $\lambda_2 = 0$ and

$$\begin{aligned} S_{1,2}^* &= \nu_1 S_1^* + \nu_2 S_2^* \\ &= F (\epsilon_{st} - \epsilon_o) Z_2 \nu_2 / T_2 \end{aligned} \quad (58)$$

where the electroneutrality condition $\nu_1 Z_1 + \nu_2 Z_2 = 0$ has been used. In a formal sense, neither E_o nor E_{st} can be measured directly, and they must be obtained from unsteady-state experiments. This requires E_t as a function of t . Combining Equations (52), (55), and (56), it can be shown readily that E_t varies with t according to

$$E_{st} - E_t = (E_{st} - E_o) g(t) \quad (59)$$

where the function $g(t)$ has been defined in Equation (52).

Figures 1–3 illustrate results of an unsteady-state experiment for 0.05m CsCl at an average temperature of $20 \pm 0.003^\circ\text{C}$. The silver, silver chloride thermocell used is shown in Figure 4. It is a sandwich cell in which the plexiglass containing the solution is sandwiched between two pure copper disks. The temperature of the electrode is measured by two single-junction copper-constantan thermocouples through the holes closely placed near the electrodes in the Cu discs. The cell length is 0.29 cm. The cell is left to equilibrate at the average temperature of 20°C for background calibration before the temperature gradient is applied. The isothermal residual e.m.f. (ideally zero) is of the order of $100 \mu\text{V}$ at the most. (In this particular example it is $34 \mu\text{V}$). This is recorded and corrected from the thermal e.m.f. After the calibration, a temperature difference of approximately 2 to 3 degrees is applied by switching the circulating water on the water jackets to hot and cold water. This is taken as time $t = 0$. The temperature difference applied is relatively small. This is because the stability of the thermal diffusion cell is governed by a set of Rayleigh numbers which are proportional to $(\text{cell length})^3 \times (\text{temperature difference})$, and the smaller this product, the better is the stability of the cell. Measurements of the e.m.f. are made with a HP3456A digital voltmeter together with a 3497A data acquisition unit interfaced to a HP85 computer. Each measurement requires less than 0.01 second and the thermal e.m.f. is measured to 0.1 microvolt.

Figure 1 records the actual warming-up of the thermocell. Here the temperature differences of the two electrodes taken every six seconds (points) were plotted against t and are fitted to an exponential function to obtain the thermal relaxation time τ . The thermal relaxation time τ

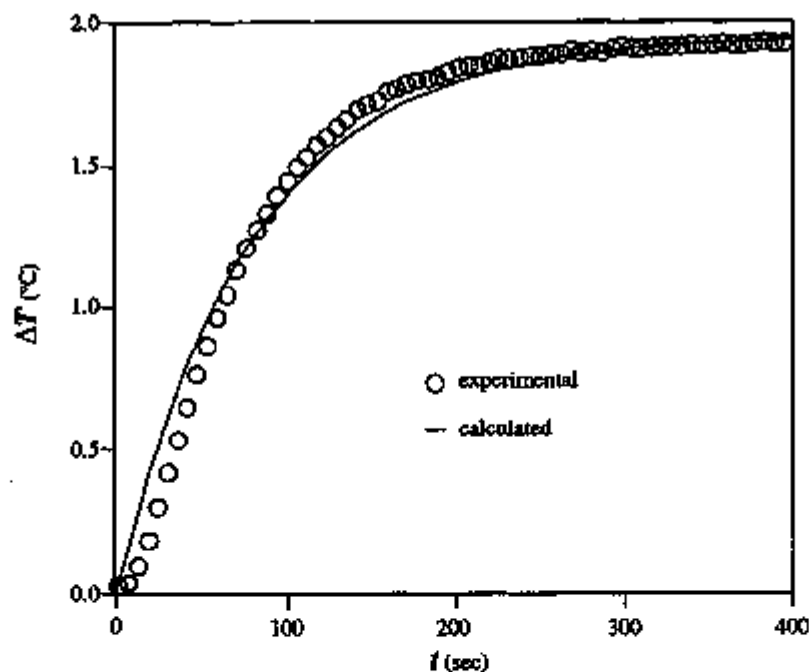


Figure 1 – Determination of the warming-up time of a Soret cell. The measured temperature difference ΔT is fitted to an exponential function to obtain the relaxation time.

depends on the cell length a and ranges from 20 sec for a cell with $a = 1$ cm to 60 sec when $a = 0.3$ cm. For a cell with a relatively large length the warming-up correction is, therefore, always in the gain-time sense, and vice versa. For the example shown here $t = 61$ sec and $t' = 56$ sec.

After the warming-up, thermal e.m.f.'s were recorded at an interval of 60 to 90 sec for at least 4 times θ . This is shown in Figure 2. For most experimental set-ups, E_s can be obtained rather accurately independent of the initial conditions. Thus E_s is first estimated by applying a standard non-linear fit of E_t to Equation (59). The value of E_s obtained is then used to construct a $\ln(E_s - E_t)$ plot vs. time to obtain the E_s value and the thermal diffusion characteristic time θ . This logarithmic plot is shown in Figure 3. It indicates a linear relationship for $t > q/2$. This is because only the $n = 1$ term makes a significant contribution to the summation in Equation (59) when $t > q/2$.

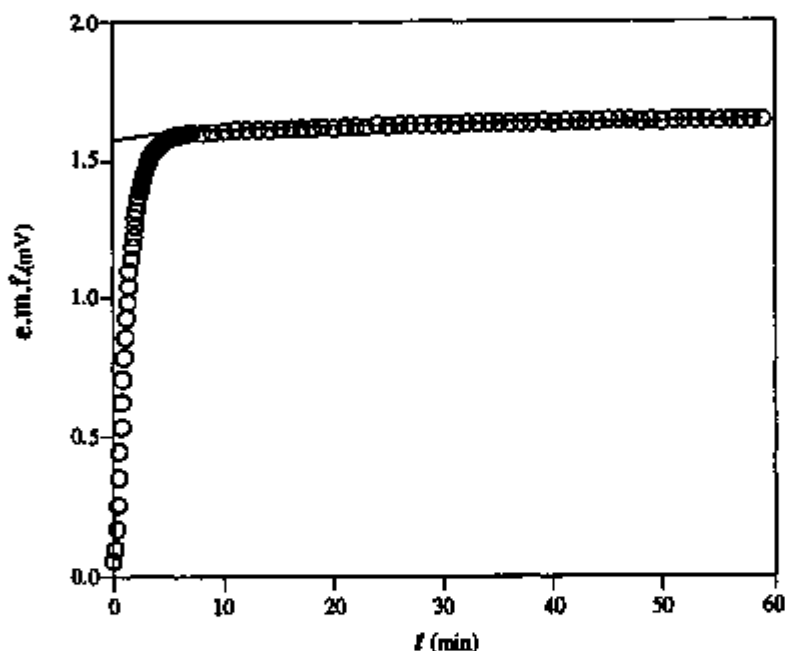


Figure 2 - Thermal emf against time during an experiment to measure the Soret coefficient of a 0.05 M CsCl solution by the potentiometric method.

The experiment described above began by applying a constant temperature gradient to the cell at an isothermal state. One may perform the reverse experiment by following changes in E_t from the Soret steady-state back to the isothermal state. The results obtained in both experiments are essentially identical [16].

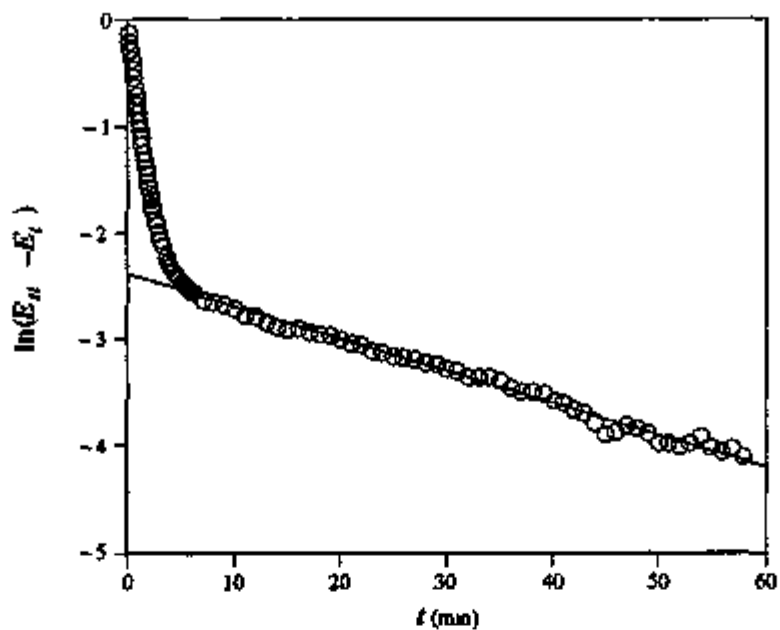


Figure 3 – $\ln(E_u - E_t)$ as a function of time for the thermal diffusion experiment with 0.05 M CsCl.

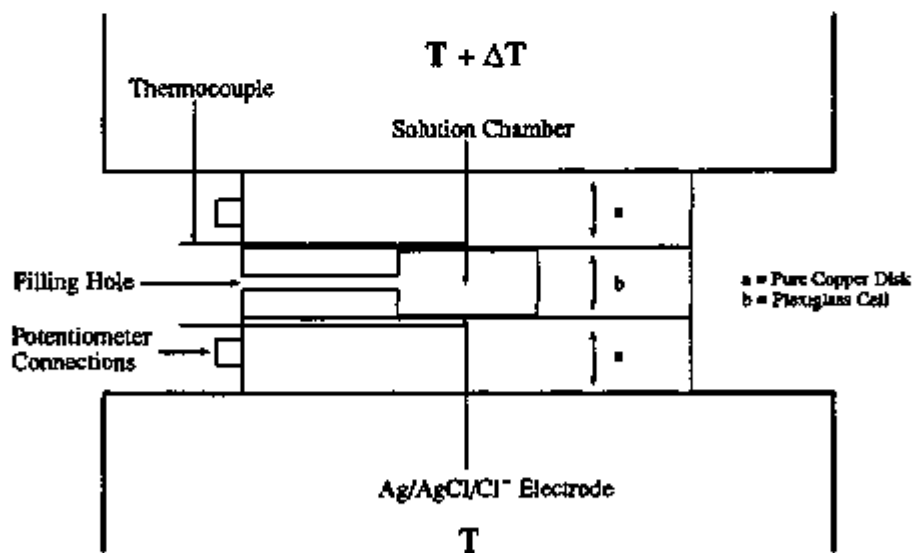


Figure 4 – The silver-silver chloride cell for determination of Soret coefficients by the potentiometric method.

Accurate values for E_0 can be obtained in a static experiment using the N-type cell shown in Figure 5. Here the electrodes are separated far enough to insure that the solution remains homogeneous during the measurements of E_0 . Values of E_0 obtained in this type of experiment agree well with unsteady-state experiments [16].

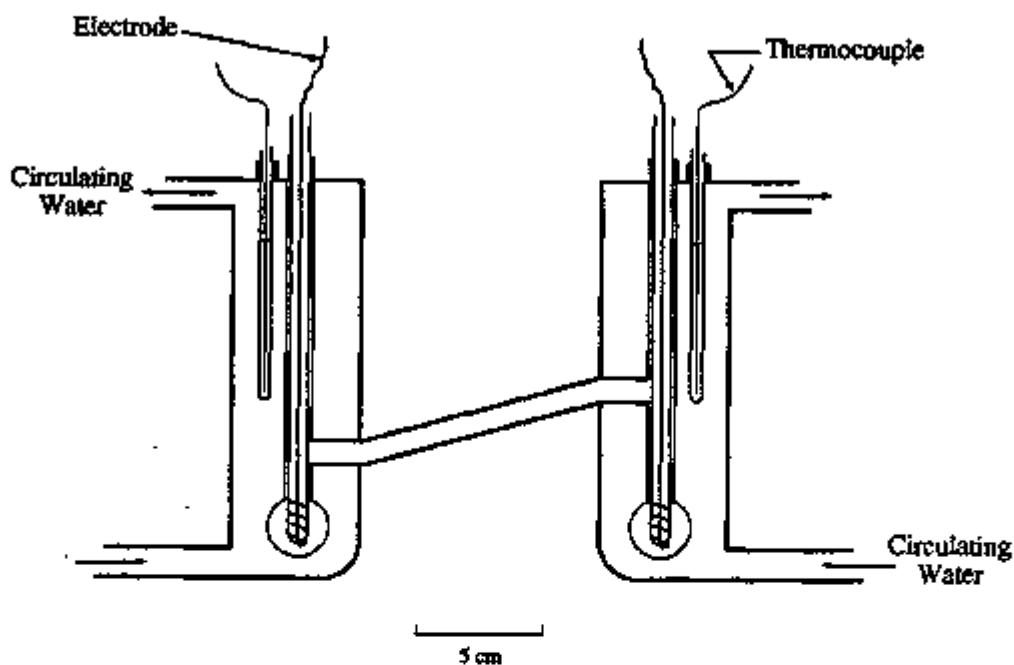


Figure 5 - An N-type cell for measurement of the initial thermal emf.

For thermocells with stable electrodes such as the silver-silver chloride or bromide thermocells, thermoelectric powers can be reproduced to within $\pm 5 \mu\text{V}/\text{deg}$. However, this does not necessarily imply that a uniform experimental accuracy can be assigned to the measured heat or entropy of transport. This is because Q^* and S^* depend on the difference $E_0 - E_0'$ as well as the transport number. For systems such as $R_2\text{NCl}$ salts where the cation transport numbers are small, the uncertainty in the S^* value can be as large as $\pm 5 \text{ JK}^{-1}\text{mol}^{-1}$ [18].

(b) The Conductimetric Method.

In the conductimetric method, the change in the concentration is followed by the change in the resistance of the solution, and the Soret coefficient is evaluated directly. The original cell used by Agar and Turner [9] is depicted in Figure 6. The end plates E' and E'' were faced with platinum foil platinized over the area in contact with the solution. A platinized Pt wire, P , inserted in the side compartment and connected with the main part of the solution through H , served as a third electrode. By pairing P with either E' or E'' , the average resistance of the solution in the lower and upper parts of the cell could be measured. Z'' and Z' were brass cylinders for circulating water from the thermostat. The cell was insulated electrically by

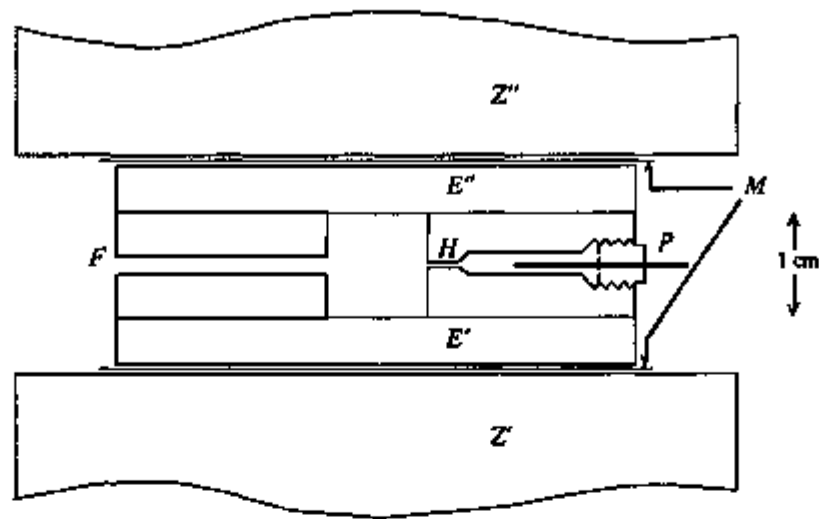


Figure 6 – The conductimetric cell used by Agar and Turner [9] for the determination of Soret coefficients.

inserting mica sheets, M , lubricated with mineral oil to ensure good thermal contact. F was the filling hole for the cell.

Denoting R' and R'' as the resistances respectively of the lower and upper halves of the cell and for $t > 0.15 \theta$, the Soret coefficient σ can be evaluated from the equation.

$$Y_t - Y_\infty = (Y_o - Y_\infty) \left(32 / \pi^2 \right) \exp(-t/\theta) \quad (60)$$

where

$$Y = (R' - R'') / (R' + R'') \quad (61)$$

and

$$Y_o - Y_\infty = -1/4\sigma \left(\partial \ln c / \partial \ln m \right)_T \Delta T \left[1 + \left(\partial \ln \Lambda / \partial \ln m \right) \right] \quad (62)$$

and Λ is the equivalent conductance of the solution. Thus by plotting $\ln(Y_t - Y_\infty)$ vs. t , $(Y_t - Y_\infty)$ can be evaluated by extrapolation to $t = 0$ (Figure 7). For short times ($t < 0.23 \theta$) Y_t is linear in t ,

$$Y_t - Y_\infty = \frac{2b_{01} \sigma \Delta T D}{a^2} \left[1 + 8i^2 \operatorname{erfc} \frac{a}{4\sqrt{Dt}} + \dots \right] \quad (63)$$

where

$$Y_t - Y_\infty = - \left[1 + \left(\frac{\partial \ln \Lambda}{\partial \ln c} \right)_T \right] \quad (64)$$

and D is the diffusion coefficient of the solution. Accordingly, σ can be deduced from the "initial" rate of change of Y_t . This is shown in Figure 8.

The conductimetric method appears to be a very accurate method even for a very dilute solution. For a 0.01M solution of a simple electrolyte, σ can be measured to within $\pm 0.01 \times 10^{-3} \text{ deg}^{-1}$.

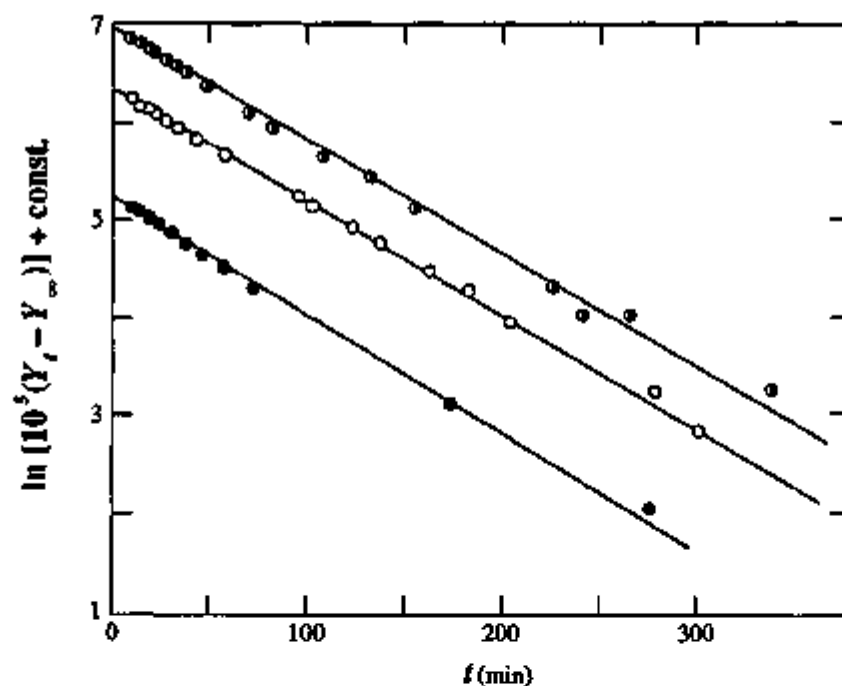


Figure 7 - $\ln(Y_t - Y_\infty)$ as a function of time for some conductimetric experiments. The upper curve, which has been displaced by a constant equal to +1, is for 0.01 M NaCl; the middle curve, not displaced (const. = 0), is for 0.01 M CsCl; and the lower curve, displaced by const. = -1, is for 0.01 M RbCl.

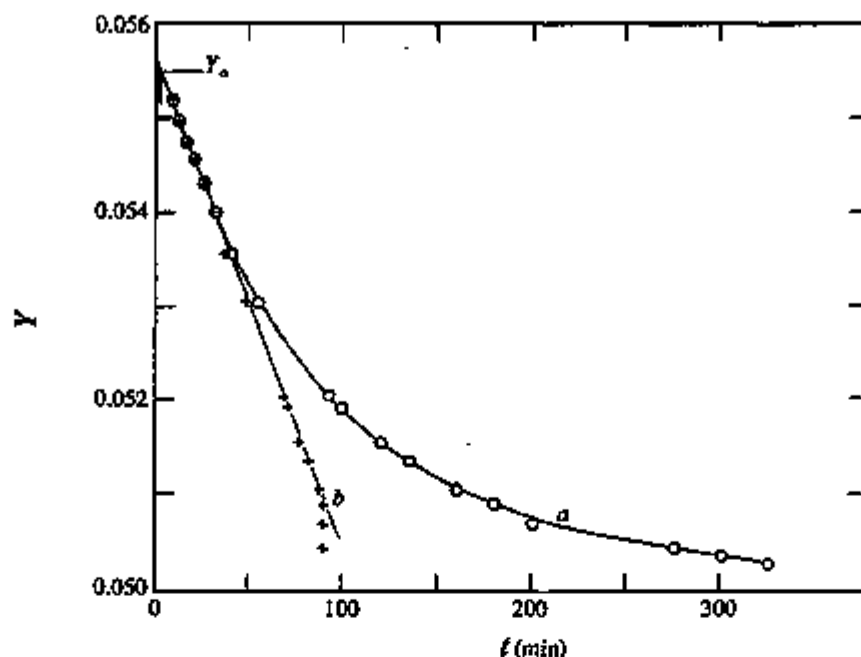


Figure 8 – The conductimetric experiment with 0.01 CsCl. Determination of the initial rate of increase of Y . The circles are values of Y plotted against time. The crosses are values of Y plotted against the function $[1 + 8i^2 \operatorname{erfc}(a/\sqrt{Dt}) + \dots]$.

(c) The Flow-Cell Method.

Figure 9 illustrates the essential features of the flow cell that was used by Thomaes [19] for measurement of Soret coefficients. The fluid mixture was passed in laminar flow between two thermostated horizontal plates. The hot and cold plates were separated by a distance of the order of 0.1 mm. The liquid, introduced at A , flowed through the cell in a horizontal direction at a flow rate such that the steady state was established before it reached the knife edge K at the opposite end. The knife edge separated the flow into hot and cold streams, designated by B and B' , respectively. By analyzing the concentrations of both streams, the steady-state concentration gradient at a given flow-rate could be derived and the Soret coefficient computed by extrapolation of the concentration gradient to zero flow rate.

The experimental parameters for a flow cell experiment can be conveniently expressed in terms of a variable X defined by the equation

$$\beta = D(Lb/a)Q^{-1} \quad (65)$$

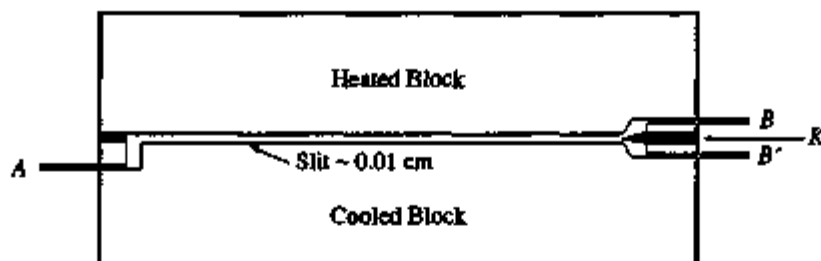


Figure 9 – Cell used by G. J. Thomaes [19] to determine Soret coefficients by the flow method.

Here D is the effective diffusion coefficient at the mean temperature, L , b and a are respectively, the length, width and depth of the flow duct and Q is the flow rate.

The thermal diffusion equation for the flow cell configuration is solved by using a variational calculus approximation [20]. The difference in the mean concentration between the cold and hot streams is found to be

$$F(\beta) = \Delta c_{\beta} / \Delta c_{\infty} = 1 - 1.045e^{-13.66\beta} + 0.026e^{-1.06\beta} \quad (66)$$

where Δc_{β} is the time-dependent concentration difference and Δc_{∞} is the limit at as β goes to infinity. Plotting $F(X)$ vs. Δc_{β} , one should thus obtain a straight line through the origin. By extrapolating this line to $\beta = \infty$ ($Q = 0$), Δc_{∞} can be deduced. The Soret coefficient σ is then given by

$$\sigma = \left(8/3 c_0 \right) \frac{\Delta c_{\infty}}{\Delta T} \Phi_{\text{solvent}}^{-1} \quad (67)$$

where Φ_{solvent} is the volume fraction of the solvent. For dilute solution $\Phi_{\text{solvent}} = 1$ and σ can be computed directly by the measurement of the initial homogeneous concentration c_0 , Δc_{∞} and ΔT , the temperature difference applied to the horizontal plates.

The flow-cell method is applicable to both electrolyte and non-electrolyte solutions, and the measurement can be carried to very dilute solutions. In a recent report by Hwang, Robinson, Billo and Lin [21], the Soret coefficient of aqueous Na_2CaEDTA solutions can be determined to within $\pm 0.01 \times 10^{-3} \text{ deg}^{-1}$ at 0.10 m ($\sigma = 5.52 \pm 0.01 \times 10^{-3} \text{ deg}^{-1}$) and to within $0.20 \times 10^{-3} \text{ deg}^{-1}$ ($\sigma = 4.75 \pm 0.20 \times 10^{-3} \text{ deg}^{-1}$) at 0.01 m.

(d) The Optical Method

The optical method follows the concentration change during thermal diffusion by analyzing the distortion of a transmitted wave from the gradient of refractive index attending the diffusion process. The method has been used widely for the measurements of the Soret coefficients of non-electrolyte mixtures as well as electrolyte solutions. By the use of the wave-front-shearing interferometry, Becsey, Bierlein and Gustafsson [22] were able to measure σ in very dilute solutions of KBr, KCl and KI in nonaqueous solvents such as formamide, N-methyl formamide and N,N dimethyl formamide.

The refractive index n in a binary mixture during thermal diffusion (under a constant one dimensional temperature gradient $(\Delta T / \Delta z)$) develops according to the Equation [23]

$$n(z,t) = n_0 + \left(\frac{\partial n}{\partial T} \right) \Delta T (z/a) + \left(\frac{\Delta T}{\Delta z} \right) K_1 \left(\frac{z}{a} - \frac{4}{\pi^2} e^{-t/\theta} \sin \frac{\pi z}{a} \right) \quad (68)$$

where n_0 is the initial uniform refractive index. Denoting x as the mole fraction of the component of the lesser molecular weight and x_0 as that of x at the initial homogeneous state, $K_1 = x_0 (1 - x_0) (\partial n / \partial x)$.

The experimental diffusion cell is usually mounted vertically. The interferogram is then taken by illuminating the cell with collimated monochromatic light. All rays are assumed to enter the sample at normal incidence. The numerical work required for the evaluation of an interferogram and the calculation of the Soret coefficient is substantial. Briefly, one analyzes the fringe shape and relates that to the optical path length of any ray leaving the cell a horizontal plane measured from the optical axis. The Soret coefficient σ can be evaluated because the path length is a function of the refractive index n , which is in turn given by σ as seen in Equation (68).

1.1.2.2 The Dufour Effect (The Diffusion Thermoeffect).

The experimental investigation of the Dufour effect is concerned with the measurement of the temperature gradient due to diffusion. The temperature distribution in a Dufour cell is time dependent. This is because the Dufour effect is gradually diminished along with the mixing process and eventually becomes negligible when the solution approaches the final homogenous solution. Thus, when two liquids at the same temperature are allowed to diffuse into each other, the temperature gradient in the system is expected to grow from zero to a maximum value and then gradually decay back to zero when the final equilibrium state is reached. For an ideal system where the heat of mixing of the two liquids is zero, the approximate value of the thermal diffusion coefficient and the heat of transport can be calculated from the observed maximum temperature gradient [24, 25] provided that the concentration gradient in the cell can also be evaluated. Since concentration changes in a Dufour cell have yet to be measured directly, thermal transport properties can only be estimated based on the measurements of the maximum temperature gradient alone.

There are two principal difficulties in the experimental investigation of the Dufour effect; namely, the large thermal conductivity of liquids and the effect of the heat of mixing. Because of the large thermal conductivity, the temperature gradient produced by the diffusion thermoeffect can quickly decay. Thus unless the system is well insulated, measurements of the temperature effect can be difficult. The effect of the heat of mixing is obvious. It contributes to the temperature effect, and thus the contribution from the heat of mixing to the observed temperature gradient must be determined. Both problems have been addressed theoretically by Ingle and Horne [26]. That the heat of transport can be obtained from the measurements of the temperature effect in a Dufour cell was first demonstrated by Rowley and Horne [27].

Figure 10 shows the experimental arrangements of Rowley and Horne for the investigation of the Dufour effect in carbon tetrachloride-cyclohexane liquid mixtures. The Dufour cell C-D is of the withdrawable liquid gate type. The upper container A serves as a container for the less dense liquid and is connected to the Dufour cell by a stopcock. The Dufour cell is filled by layering the denser liquid beneath H_2O . Since water has a negligible solubility in either carbon tetrachloride or cyclohexane, it serves as an ideal third liquid which, when withdrawn from liquid gate F, will permit the two liquids to form a sharp boundary without turbulence and also at a well-defined initial time. Both the upper and the lower sections are thermally equilibrated with the thermostating jackets surrounding them. The experiment begins by slowly withdrawing water through F. This permits the liquid in the upper reservoir to gradually replace water and finally, when the water is completely withdrawn, a sharp interface between the two liquids is formed. At the instant of formation of the interface the circulating water in the lower jacket (around the Dufour cell) is quickly evacuated to create an adiabatic condition during the measurement of the temperature effect.

The change in temperature in the Dufour cell is monitored through thermocouple D in the cell. By measuring the temperature responses as a function of the position and time and using

the temperature data in conjunction with a solution of the energy transport equation (in the mass frame of reference),

$$\begin{aligned} \rho c_p \left(\frac{\partial T}{\partial t} \right) &= \nabla \cdot \vec{J}_q = -\nabla \cdot \vec{J}'_q - \sum \vec{J}'_i{}^m H_i \\ &= -\nabla \cdot \vec{J}'_q - \sum \vec{J}'_i{}^m \cdot \nabla (H_i - \bar{H}_r), \quad i \neq r \end{aligned} \quad (69)$$

solved subject to experimental boundary conditions, a best nonlinear, least square estimate of the Onsager coefficients L_{ij} (and hence Q_i^*) can be obtained. In Equation (69) ρ is the density and c_p is the specific heat capacity of the mixture. For the carbon tetrachloride-cyclohexane system at 1 atm, ρ and C_p are known as a function of the composition of the mixture. \bar{H}_i is the partial specific enthalpy of component i . For a mixture with two components 1 and 2, $\bar{H}_1 - \bar{H}_2$ can be obtained from the heat of mixing data. Also, in Equation (69) a relatively small entropy source term for the bulk flow is ignored and the pressure of the system is assumed constant.

Figure 10 - Cell used by Rowley and Horne [27] to investigate the Dufour effect in liquids.

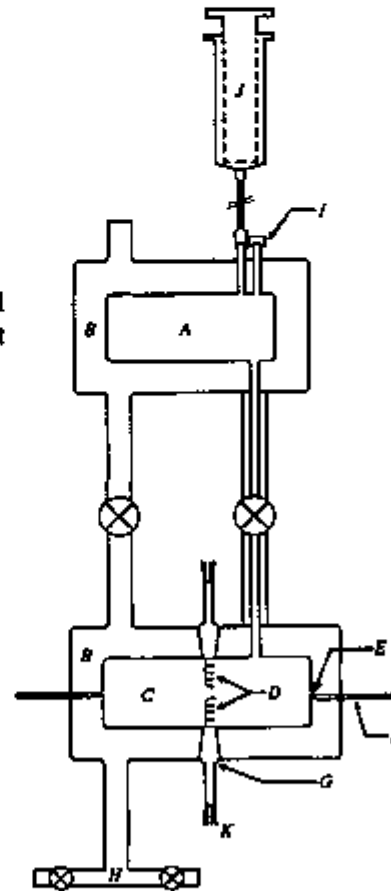


Figure 11 shows the temperature difference between positions $z/a = 0.4$ and $z/a = 0.6$ observed by Rowley and Horne for a mixture where the initial mole fractions of CCl_4 are 0.0179 and 0.804, respectively, for the fluids in the upper and lower layers. The initial interface is formed at $z/a = 0.5$. Here z is the vertical axis and a is the cell length. The data points (dots) are compared with the theoretical predictions from the solution of the energy transport equation,

$$\begin{aligned} \bar{C}_p \left(\frac{\partial T}{\partial t} \right) = & \bar{V} \kappa \frac{\partial^2 T}{\partial z^2} + \bar{V} \left(\frac{\partial T}{\partial t} \right) \left(\frac{\partial \kappa}{\partial z} \right) + D \left(M_2 Q_1^* / M \right) \left(\frac{\partial^2 x_1}{\partial z^2} \right) \\ & + D \left(\frac{\partial^2 \bar{H}^E}{\partial x_1^2} \right)_{T,P} \left(\frac{\partial x_1}{\partial z} \right)^2 + D \left(\frac{\partial x_1}{\partial z} \right)^2 \left[\frac{\partial \left(M_2 Q_1^* / M \right)}{\partial x_1} \right]_{T,P} \end{aligned} \quad (70)$$

subject to adiabatic (full line) and diathermic (dashed line) boundary conditions. In Equation (70) \bar{C}_p is the molar heat capacity, \bar{V} is the molar volume, x_1 is the mole fraction of component 1 (taken to be CCl_4), M_i is the molecular weight of i , $M = x_1 M_1 + M_2 x_2$ is the

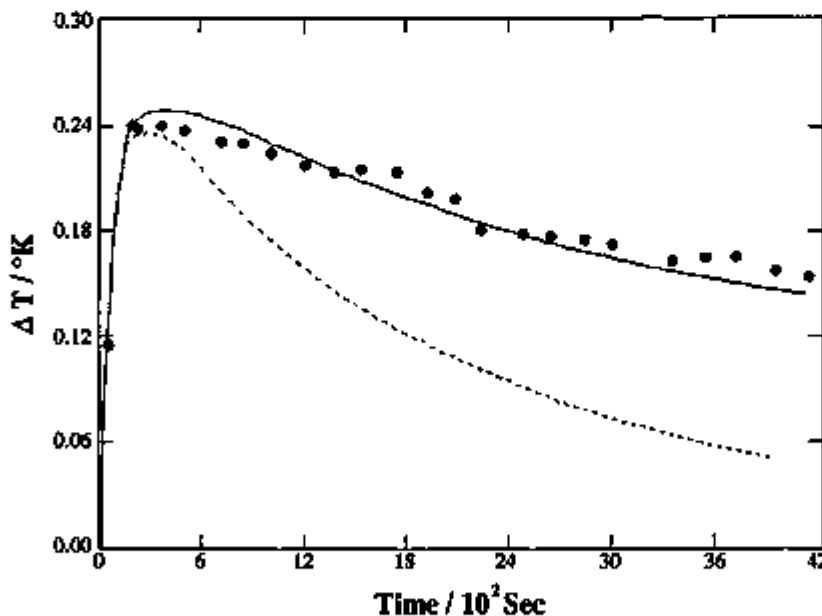


Figure 11 – Temperature difference ΔT as a function of time for a Dufour experiment with a carbon tetrachloride-cyclohexane mixture.

weighted molecular weight of the mixture, κ is the thermal conductivity and H^E is the excess molar enthalpy. As expected, Figure 11 indicates that ΔT decays rapidly for a diathermic boundary condition. The maximum temperature difference observed is approximately 0.24°K . It turns out that when the thermocouples are symmetrically placed with respect to the initial interface, the heat of reaction contributes rather insignificantly to the observed temperature difference. This is because of the symmetric nature of the heat of mixing arising due to the fact that the mass frame of reference is used for the diffusion fluxes and thus the two fluxes are mutually against each other ($\vec{J}_1^m = -\vec{J}_2^m$). The data reported according to the authors are the values of $Q_{\text{CCl}_4}^*$ which provides the best fit for Equation (70) and the experimental ΔT . Since the data are evaluated with \vec{J}_i^m it seems that the data reported are really the values of $Q_{\text{CCl}_4}^* - Q_{\text{C}_6\text{H}_6}^*$.

Rowley and coworkers [28, 29] investigated the diffusion thermoeffect in ternary liquid mixtures. They extended the theoretical work of Ingle and Horne to obtain an analytical expression for ΔT when the thermocouples are placed symmetrically with respect to the initial interface. For a system with reasonably constant thermophysical properties, the temperature difference $\Delta T(z')$ between two points at an equal distance z' from the initial interface is

$$\Delta T(z') = \left(4\pi/a^2\bar{C}_p\right) \sum_{i=1}^2 \left[\left(Q_1^* D_{1i} + Q_2^* D_{2i} \right) \Delta w_i / \left(\theta_{ii}^{-1} - \tau^{-1} \right) \right] \cdot \sum_{l=1}^{\infty} F_{il} \sin \left[(2l-1)\pi z' / a \right] \quad (71)$$

where D_{ij} is the mutual diffusion coefficient, Δw_i is the initial difference in the mass fraction of component above and below the interface and θ_{ij} is the thermal diffusion characteristic time, $\theta_{ij} = a^2 / \pi^2 D_{ij}$. Also denoting κ as the thermal conductivity

$$\tau = \rho c_p a^2 / \pi^2 \kappa \quad (72)$$

and

$$F_{il} = \left\{ \exp \left[-(2l-1)^2 t / \theta_{ii} \right] - \exp \left[-(2l-1)^2 t / \tau \right] \right\} / (2l-1) \quad (73)$$

In Equation (71), Q_1^* and Q_2^* can be treated as two simultaneously adjustable parameters. Two experiments at different initial conditions must be performed at each mean composition to decouple the parameters. Again, because of the mass frame of reference used, Q_1^* and Q_2^* are strictly the relative heats of transport $Q_1^* - Q_3^*$ and $Q_2^* - Q_3^*$, respectively.

1.1.3 Experimental Data and Discussion

Thermal diffusion and the diffusion thermoeffect are the results of the coupling of matter and heat transport. Eastman argued that the matter transport due to the relative motion of particles may result in a change in the (local) intensity of intermolecular forces and the adjustment occasioned by such changes may result in a finite heat effect. Therefore, in a thermal diffusion experiment when a solute particle is transported between regions of differential temperature difference in a stationary solvent, a quantity of heat is absorbed from the heat reservoir behind and given out ahead of the moving particle. This heat is the heat of transport Q^* of the particle. This picture clearly suggests that thermal diffusion data will be useful in the investigation of the nature of interaction in solutions and perhaps especially in those areas where dynamics and the structure are involved.

Experimental data before 1963 have been reviewed by Agar [17] and Tyrrell [11]. The data surveyed here are recent ones. The survey will not be exhaustive, and only those data which will help to illustrate interesting aspects of the study of the Soret and Dufour effects will be discussed.

There is a simple picture for the heat of transport and the diffusion thermoeffect. The temperature surrounding a moving particle is generally not uniform. One way to see this is to recognize the possibility that the molecules in front of a moving particle are "pressured" by the approaching particle and therefore compressed. Conversely, the fluid molecules behind a moving particle are expanded. Since compression of fluids usually results in heating and vice versa, the temperature ahead of a moving particle is higher than the temperature behind it. Consequently, if an isothermal condition is applied, heat is evolved ahead and absorbed behind the moving particle. In a stationary state a heat flux is observed in the same direction as the diffusion flux. This is the diffusion thermoeffect. The heat flux in the diffusion thermoeffect is opposite to the conduction heat current that flows from a region of high temperature to a region of low temperature.

When positive heat is evolved ahead, and absorbed behind, a moving particle, convention assigns a positive sign to the heat of transport of the particle. In the same way, when entropy is evolved ahead and absorbed behind, the entropy of transport S^* is positive. When entropy is absorbed behind the particle to keep the temperature constant, the particle is obviously a net "structure-maker". However, if entropy is evolved behind the moving particle, the particle is a "structure-breaker". Thermal diffusion data are therefore expected to reflect structural effects induced by the moving particle.

In an effort to provide a theoretical interpretation for Q^* and S^* , Agar [17] proposed a hydrodynamic theory for the heat of transport. The similarity between the heat sink and source surrounding a moving particle and the existence of the electrical charge sink and source in a dipolar molecule led Agar to suggest that the moving particles are surrounded by "thermal dipole moments". Agar, Mou and Lin [5] have calculated the thermal dipole moment and show

that, indeed, the heat of transport can be given in terms of the thermal polarization. The hydrodynamic expression for the standard single-particle heat of transport at infinite dilution is

$$Q_i^{*o} = \left(4\pi T/3\right) \int \left(\frac{\partial S}{\partial r}\right) f(r) r^3 dr \quad (74)$$

where $S = S(r)$ is the entropy density at a distance r from the particle of interest, and $f(r)$ is a function describing the velocity field of the solvent induced by the motion of the particle ($f(r) = 1$ at $r = \infty$, and $f(r) = 0$ at the surface of the ion). The expression of Q_i^{*o} given in Equation (74) is obtained by immersing a single particle in its solvent, which is regarded as a hydrodynamic continuum. The significance of the result lies in the fact that the relationships between the heat of transport and the structure (through $\partial S/\partial r$) and dynamics [through the function $f(r)$] are clearly stated. It indicates that if there are no polarizable structures surrounding the particle, i.e., in case $(\partial S/\partial r) = 0$, Q_i^{*o} will be zero.

Systematic measurements of the heats of transport of dilute aqueous electrolyte solutions have been reported using the silver-silver halide electrodes at 25°C. For 1:1 electrolytes, data available include alkali chlorides [30] and bromides [31], ammonium and tetraalkylammonium chlorides [32], and hydrochloric acid [15]. For 2:1 electrolytes there are data for nickel and alkaline earth chlorides [33], and for 3:1 electrolytes, data are available for rare earth chlorides [34]. The limiting law for the concentration dependence of the molar heat of transport is [35].

$$\begin{aligned} Q_{+-}^* &= v_+ Q_+^* + v_- Q_-^* \\ &= Q_{+-}^{*o} - \alpha(\bar{H}_{+-})\Gamma - \frac{2e^2}{3\epsilon k_B T} (v_+ Z_+^2 + v_- Z_-^2)\Gamma \\ &\quad + \left(v_+ v_- / v_+ + v_-\right) (R_+^s - R_-^s) (\bar{H}_+^o - \bar{H}_-^o)\Gamma \end{aligned} \quad (75)$$

where $\Gamma = \sqrt{(4\pi e^2 \sum c_i Z_i^2 / k_B T \epsilon)}$ is the reciprocal Debye length and R_i^s is the Stokes law radius of i . The second term in the right-hand side of the second equality $\alpha(\bar{H}_{+-})$ is the limiting slope for the partial molar heat content. The third term is due to the direct ion-ion electrostatic interaction, and the last term is due to the electrophoretic effect. Because the ion-ion term describes the effect due to the ionic atmosphere and can be obtained from the Debye-Hückel equilibrium pair-distribution function, this term, together with the enthalpy term, have been referred to as the thermodynamic contribution to the limiting law of the molar heat of transport.

The electrophoretic contribution to the limiting slope must be estimated because absolute ionic values for \bar{H}_i are not available. For most systems, however, it is small. This is because this

contribution is proportional to the product of the differences in the Stokes law radii and the transported enthalpy. In fact, for electrolytes such as KCl where $R_{K^+}^s = R_{Cl^-}^s$, the electrophoretic effect is negligible. Figure 12 describes the concentration dependence of S_{CsCl}^* at 20°C [36]. The line gives the least mean square fit of the experimental data (excluding the results of two most dilute solutions). The slope of the line is -34.2 (in $J mol^{-1}K^{-1}m^{-1/2}$). The theoretical ion-ion electrostatic limiting slope is -35.2 .

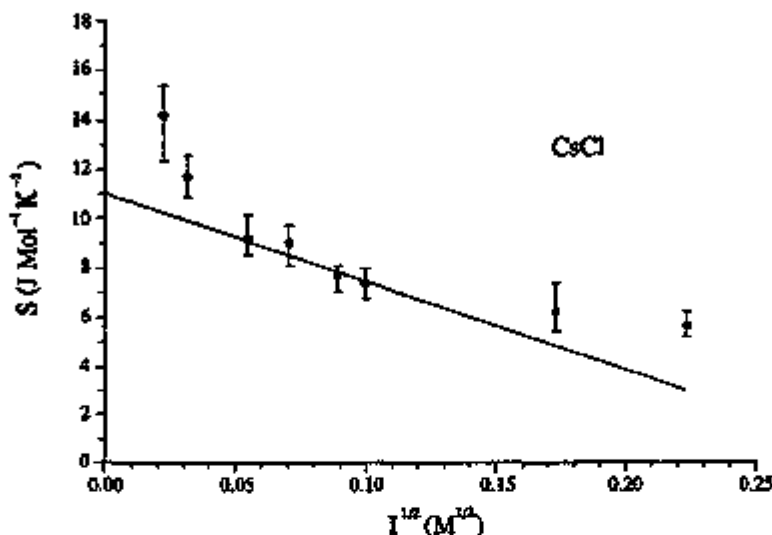


Figure 12 - The effect of concentration on the entropy of transport of CsCl at 20°C.

In comparing experimental data with the result given in Equation (74) Q_{ion}^{*o} and S_{ion}^{*o} must be estimated from the molar quantities Q_{\pm}^{*o} and S_{\pm}^{*o} , respectively. There are a number of ways that this can be accomplished. One approach proposed by Takeyama and Nakashima [37] is based on exploiting the consequences resulting from decomposing the experimental molar heat of transport into the ionic heats of transport in the laboratory frame. (As discussed earlier, although the molar heats of transport are independent of the frame of reference, the same is not true for the ionic heats of transport). Their method (known as the reduction rule) yields $Q_{Cl^-}^{*o} = 0.53$ kJ/mol which is close to $Q_{Cl^-}^{*o} = 0.37$ kJ/mol based on the Gurney scale [38]. Table 1 lists standard single-ion heats of transport at infinite dilution according to the reduction rule of Takeyama and Nakashima. The experimental data are taken from references [30-34] and also from Takeyama and Nakashima [37].

We shall use data given in Table 1 to infer structural effects of the ions. Since structure-makings and structure-breakings in aqueous electrolyte solutions refer commonly to those effects that are added to the simple ion-dipolar interaction, we shall take a spherical Born ion with a slipping surface as a structurally neutral reference ion. For a Born reference ion with a

slipping surface, the entropy density around the ion is given by the Born theory of hydration and Equation (74) can be integrated [5] to give,

$$Q_{\text{Born}}^{*o} / Z_i^2 D_i = 2.20 \cdot 10^{12} \text{ J sec/mol m}^2 \quad (76)$$

where D_i is the self-diffusion coefficient, which is related to the hydrodynamic radii R_i in Equation (75) through the Stokes-Einstein relationship and which can also be deduced from the ionic equivalent conductance according to the Nernst equation [39]. The result given in Equation (76) can now be compared with the values of $Q_i^{*o} / Z_i^2 D_i$ listed in Table 1. Take the alkali metal ions for example. Na^+ is a weak structure-maker, because $Q_{\text{Na}^+}^{*o} / D_{\text{Na}^+} = 2.60 \cdot 10^{12}$,

Table 1 – The Single Ion Heat of Transport at Infinite Dilution

Ion	$D \cdot 10^9$ (m^2/sec)	Q_i^{*o} (10^3 J/mol)	$10^{-12} Q_i^{*o} / Z_i^2 D_i$ (J sec/mol m^2)
H^+	9.31	13.3	1.43
Li^+	1.03	0.53	0.51
Na^+	1.33	3.46	2.60
K^+	1.96	2.59	1.32
Rb^+	2.07	3.91	1.89
Cs^+	2.08	4.01	1.93
NH_4^+	1.95	1.73	0.89
Me_3N^+	1.20	10.00	8.33
Et_3N^+	0.87	14.29	16.43
$n\text{-Pr}_3\text{N}^+$	0.62	18.36	29.61
$n\text{-Bu}_3\text{N}^+$	0.51	20.79	40.76
Ag^+	1.65	6.37	3.86
Tl^+	1.99	4.33	2.18
Mg^{+2}	0.71	9.04	3.20
Ca^{+2}	0.79	9.8	3.10
Sr^{+2}	0.79	11.1	3.52
Ba^{+2}	0.85	12.4	3.66
Ni^{+2}	0.71	9.3	3.30
La^{+3}	0.62	19.5	3.49
Sm^{+3}	0.61	19.6	3.57
Yb^{+3}	0.58	18.3	3.51
OH^-	5.32	17.2	3.14
F^-	1.47	3.93	2.67
Cl^-	2.03	0.53	0.26
Br^-	2.08	0.60	0.29
I^-	2.04	-1.55	-0.76
NO_3^-	1.90	-0.63	-0.33
ClO_4^-	1.81	-0.31	-0.17
IO_3^-	1.45	2.00	1.38

which is slightly larger than the value for the reference ion. In comparison, all other alkali metal ions carry smaller values and are structure-breakers. Following the same analysis, tetraalkylammonium ions are strong structure-makers as the result of the hydrophobic interactions. The structure promoting effect of the lanthanide ions has led Frank and Evans [40] to postulate the existence of a super-lattice structure around the lanthanide ions, generally referred to as the iceberg effect. Here, the heat of transport data also indicate that they are structure-makers. The halide ions show an expected trend, that is the F^- ion, the smallest ion in the group, is a structure-maker, and I^- , the largest halide ion listed, is a structure-breaker. However, it is somewhat surprising to find that the smallest alkali metal ion Li^+ is a structure-breaker. According to Chakroborty and Lin [41], the reason that Li^+ is a structure-breaker is the exchange effect. The strong ion-dipolar interaction is likely to give Li^+ an extended hydration cosphere resulting in a large hydrated ion for Li^+ . Thus water molecules in the outer hydration cosphere may undergo exchanges with the molecules in the bulk when the Li^+ ion diffuses. Exchanges create disorder and Li^+ , therefore, is a structure-breaker.

The heat of transport generally measures effects taking place not in the close vicinity of the particle, but those that are occurring at a distance from the particle. This is clearly indicated in Equation (74). Since $f(r=R_p) = 0$ and $(\partial S/\partial r) = 0$ at $r = \infty$, the integrand grows from zero at $r = R_p$ to a maximum, and eventually must decay to zero at $r = \infty$. For a slipping Born ion, the maximum occurs at $r = 1.5R_p$. For an ordinary ion with $R_p = 2\text{\AA}$, the predominant contributions to the integral are from regions around $4\text{--}3\text{\AA}$.

Investigation of the temperature dependence of the thermal diffusion properties may also give interesting insights into the nature of interaction in solutions. For 0.01m alkali chlorides in H_2O and D_2O , both σ and $d\sigma/dT$ have been measured by Wood and Hawksworth [42] using the conductimetric method. Their results in H_2O have been summarized below, assuming that σ varies linearly with temperature.

$$\sigma (LiCl) = 9.9 \cdot 10^{-3} (t-25.1) \quad (77)$$

$$\sigma (NaCl) = 0.091 \cdot 10^{-3} (t-2.8) \quad (78)$$

$$\sigma (KCl) = 0.107 \cdot 10^{-3} (t-11.6) \quad (79)$$

$$\sigma (RbCl) = 0.111 \cdot 10^{-3} (t-4.1) \quad (80)$$

$$\sigma (CsCl) = 0.111 \cdot 10^{-3} (t-4.1) \quad (81)$$

where t is temperature in $^{\circ}C$. It is seen that $d\sigma/dT$ for $LiCl$ is unusually small and may indicate the structural effect discussed above. That is, if the exchange of water molecules between the hydration cosphere and the bulk is the principal reason for the small heat of transport observed, then the temperature data indicate that the exchange is not sensitive to change in the temperature. Values of $d\sigma/dT$ for the other salts are comparable. What is significant here, however,

is the "transition temperature" that is predicted. For NaCl, σ , and consequently Q_{NaCl}^* , changes sign from positive to negative at 2.8°C. Similarly, Q_{KCl}^* changes sign at 11.6°C and Q_{RbCl}^* at 4.1°C. The results are remarkable in view of the fact that the maximum density of H₂O occurs at 4°C and at this temperature $(\partial P / \partial T)_V$ changes sign from positive to negative. Compression of the fluid ahead of, and expansion behind, the moving particle will generally cause the temperature to be higher ahead and lower behind resulting in a positive heat of transport for the particle. The situation is just the opposite for H₂O below 4°C where $(\partial P / \partial T)_V < 0$. Consequently, the heat of transport is expected to reverse its sign around 4°C if indeed the compression and expansion contribute significantly to the heat of transport. For D₂O, where the temperature for the maximum density is at 11.2°C, Woodward and Hawksworth's data predict a "transition temperature" for Q_{NaCl}^* at 16.4°C, Q_{RbCl}^* at 18.1°C, and Q_{CsCl}^* at 18.3°C.

Since $(\partial P / \partial T)_V = (\partial S / \partial V)_T$, the heat of transport can be viewed from yet another angle by inference from the entropy changes due to changes in volume induced by diffusion. Tyrrell [43] first noticed this and argued that when an ion is displaced, the void volume left behind must be reoccupied by the solvent molecules nearby. Further, when the Hittorf flux is adopted, the number of solvent molecules reoccupying the void volume must be exactly identical to the number of solvent molecules carried away by the ion, i.e., the hydration number n_h in aqueous solution. The entropy change associated with this is ΔS ,

$$\Delta S = \left(\frac{\partial S}{\partial V} \right)_T \left[n_h \bar{V}_{\text{H}_2\text{O}}^0 - (n_h \bar{V}_{\text{H}_2\text{O}} + V_{\text{ion}}) \right] \quad (82)$$

which will contribute to the entropy of transport. In Equation (82) $\bar{V}_{\text{H}_2\text{O}}^0$ and $\bar{V}_{\text{H}_2\text{O}}$ are, respectively the molar volume of H₂O in the bulk and in the hydration cosphere, and V_{ion} is that of the bare ion. A group of ions that is particularly suitable for testing the present hypothesis is the tetraalkylammonium ions. Because of the hydrophobic interaction, n_h is very small or nearly zero. Thus if ΔS should make a significant contribution to the heat of transport, a correlation between Q_i^* and R_i^3 is expected. Table 2 gives a summary of Q_i^* listed in Table 1 and the ionic radii R_i taken from Stokes and Robinson [39] for ammonium and tetraalkylammonium ions. The correlation found in this table, though not quantitative, is striking.

Table 2 - The Standard Ionic Heats of Transport and the ionic radii R_i

	$R_i(\text{\AA})$	Q_i^* (kJ/mol)	$Q_i^*/Q_{\text{NH}_4\text{N}^+}^*$	$R_i^3/R_{\text{NH}_4\text{N}^+}^3$
H ₄ N ⁺	1.48	1.73	0.17	0.08
Me ₄ N ⁺	3.47	10.00	1	1
Et ₄ N ⁺	4.00	14.23	1.42	1.53
n-Pr ₄ N ⁺	4.52	18.36	1.84	2.21
n-Bu ₄ N ⁺	4.94	20.79	2.08	2.89

Equation (74) is derived based on the consideration of heat sink and source around a moving particle. It is, therefore, a general expression which should be applicable also to non-electrolytes. Although the same level of discussion for non-electrolyte solutions is not quite ready primarily because large volumes of systematic data are yet to be accumulated, there are several interesting non-electrolyte systems which have been investigated for some specific purposes. Two examples are discussed below.

Thermal diffusion factors ($T\sigma$) for binary mixtures of alcohols and aromatic hydrocarbons with carbon tetrachloride were measured, using the optical method, by Belton and Tyrrell [44], Farsang and Tyrrell [45] and Anderson and Horne [46] and by Story and Turner [47] using the flow-cell method. Beyerlein and coworkers, using the thermogravitational thermal diffusion column, extended the investigations to other compounds [48–51]. These included chloroform with acetone and aromatic hydrocarbons, and also the ^2H thermal diffusion isotope effect in benzene and methanol. More recently, Rutherford used the thermal diffusion column to determine thermal diffusion effects for isotopic substitutions in benzene, substituted benzenes and carbon disulfide [52–54]. (We have not discussed the thermal gravitational thermal diffusion method because in this method the separation observed is enhanced by the bulk flow and not by pure thermal diffusion alone. When thermal diffusion column measurements are done with great care and precision, good results can be obtained. However, in many studies there arise questions regarding conformance of the experiments to the ideal conditions assumed in the derivation of the theory of the thermogravitational process. In such circumstances, results are frequently produced that can not be confirmed by other independent methods [55].

Thermal diffusion factors are sensitive to the composition of solutions and are useful in studying the molecular association reaction and complex formation. For the methanol-benzene and ethanol-toluene mixtures, the thermal diffusion factor is found to increase from negative values at high alcohol concentrations to positive values when the alcohol concentration is decreased. It approaches a maximum and then gradually decreases at lower alcohol concentrations. This concentration behavior is due to the self-association of the alcohol component and can be interpreted with the molecular association theory of Baranowski, deVries, Haring and Paul [56] or with the modified form of this theory due to Johnson and Beyerlein [48]. For some chloroform mixtures, where the molecular attraction between chloroform and the other component is much stronger than the two chloroform molecules, complex formations have been observed. For example, in the chloroform-acetone system, the mixtures contain 1:1 chloroform-acetone complex as well as a small amount of 2:1 complex. The intermolecular attraction between chloroform and benzene is found to be very strong and a 2:1 chloroform-benzene complex has been observed. The molecular interaction energy between chloroform and a benzene molecule estimated from the temperature dependence of the thermal diffusion factor is 4.60 kJ, which is in good agreement with the other independent estimate [57].

That thermal diffusion studies can be sensitive to molecular association reactions was pointed out many years ago by Wagner [58]. Wagner developed a simple theory of diffusion for dilute solutions in which the solute A consists of two isomeric species A' and A'' in equilibrium

with one another. When the equilibrium $A' \rightleftharpoons A''$ is attained rapidly (in comparison with the time scale of the diffusion), Wagner showed that the application of a temperature gradient will cause A to migrate, thereby increasing the concentration $A = A' + A''$ at one end of the cell and decreasing it at the other (thermal diffusion) and that diffusion under isothermal conditions will cause enthalpy flow, in addition to that associated with the partial molar enthalpy of A , i.e., the heat of transport. An exact thermodynamic treatment of the "Wagner effect" has been given by Agar and Lin [7]. They showed that the heat of transport derived from the Dufour and Soret effects are identical. Accordingly, the reciprocity relation is confirmed for the Onsager phenomenological coefficient for heat-matter coupling. Agar and Lin's treatment can be extended readily to equilibria such as $AX \rightleftharpoons A^+ + X^-$, and it suggests that the existence of such an equilibrium will give rise to an additional contribution to the heat of transport of a weak electrolyte when the rate of dissociation is around 50%. However, the additional heat of transport is proportional to the enthalpy of dissociation, and in a typical example such as a weak acid, the enthalpy of dissociation is small so that this additional heat of transport may be too small to be observed.

The heats of transport from the diffusion thermoeffect in ternary mixtures of toluene-chloroform-bromobenzene reported by Platt, Vongvanich, Fowler, and Rowley [28, 29], were re-investigated as binary mixtures by Rowley and Hall [59]. They show that the ternary data can be estimated from the binary results. We pointed out that the heats of transport measured in the diffusion thermoeffect experiments are the relative heats of transport. Consequently, comparisons of the diffusion thermoeffect results with results obtained by other methods based on \bar{J}_i^H require caution. However, at the infinite dilution limit, the heat of transport of the solvent component approaches zero so that the "pure component" heat of transport obtained at this limit is independent on the solvent component. Yi and Rowley [60] reported the molar heat of transport of carbon tetrachloride in benzene, toluene, 2-propanone, n-hexane and n-octane at 298.15 and 308.15°K at ambient pressure. At 298.15°K, values of $Q_{\text{CCl}_4}^*$ found are within 1.46 to 2.16 kJ/mol. and at 308.15°K, within 1.54–1.86 kJ/mol.

Yi and Rowley [61] tested the existing theories of thermal diffusion using results obtained from diffusion thermoeffect measurements. The theories tested were the Brownian motion theory of Bearman, Kirkwood and Fixman [62], the thermodynamic theory of Guy [63], the transition state theory of Mortimer and Eyring [64], the revised Enskog theory of Barajas, Garcia-Collin and Pina [65] and the kinetic theory using the square-well model potential of McLaughlin and Davis [66]. Although none of the theories tested were able to provide even qualitative agreement with experiment, the square-well Enskog theory seems capable of providing approximate agreement with experimental data by adjusting the potential parameters for the mixtures. Yi and Rowley demonstrated the validity of the frequently expressed view that thermal diffusion properties are sensitive to the interaction potentials. Theory with a realistic potential energy model will be required for the discussion of thermal diffusion properties at the molecular level.

1.2 Thermal Diffusion in Gases

The phenomenon of thermal diffusion is a second order effect which did not appear in the kinetic theory of gases developed by workers in the nineteenth century. It was first recognized by David Enskog [67] at the University of Uppsala in 1911 when he presented the kinetic theory for the special case of a Lorentzian gas, observing that a mass motion, or flux, of particles could be caused by a thermal gradient as well as a concentration gradient. In his doctoral dissertation, Enskog [68] propounded the theory for the general case and gave an explicit expression for the coefficient of thermal diffusion. Working independently, and at about the same time, Sidney Chapman [69] obtained a similar result and then proceeded to verify it experimentally [70]. The fact that the nineteenth century workers overlooked this is primarily due to its being a non-equilibrium effect and furthermore the coefficient is identically zero for the Maxwellian molecule, which was the popular molecular model of that era. In reality the molecular interaction is much more complicated and a "unique and correct" analytical form is still not known. The method of Chapman and Enskog proceeds through solving the Boltzmann Equation with a perturbed Maxwellian velocity distribution (the non-equilibrium case) and expresses the phenomenological coefficients in terms of "collision integrals". These collision integrals are expressed in terms of the intermolecular forces and molecular weights. The mathematical and numerical procedures are very complicated and difficult to execute.

While the initial discovery of thermal diffusion in gases evolved through the development of the rigorous kinetic theory, the derivation of the phenomenological coefficients from non-equilibrium thermodynamics is a very illustrative approach. This method has the advantage of formulating the transport coefficients directly in terms of the experimental parameters and produces the defining equations for the transport coefficients, several of which have been given explicitly in the introductory section of this report. Equation (11) in that section states that the fundamental driving force for diffusion is the negative gradient of chemical potential divided by T . For gases the composition scale usually chosen is the molar concentration, c_j , or equivalently the mole fraction, x_j . The variation of chemical potential at constant pressure and given temperature is

$$\left(d\mu_j\right)_{P,T} = \left(\partial\mu_j/\partial C_j\right)_{P,T} dC_j \quad (83)$$

or

$$\left(d\mu_j\right)_{P,T} = \left(\partial\mu_j/\partial x_j\right)_{P,T} dx_j \quad (84)$$

The mass fractions, $w_j = \rho_j/\rho$, are related to the molar concentration or mole fractions, $c_j, x_j = N_j/N$, through the expression for the mass density

$$\rho_j = M_j N_j \quad (85)$$

For a binary system, the definitions of the thermal diffusion ratio, k_T , and the thermal diffusion factor, α_T , that quantity which is to be measured by the following experimental methods, are defined by the condition $\vec{J}_1 = -\vec{J}_2 = 0$, the steady state, where the mass flux is zero but the heat flow is not zero. Thus

$$D_{12} \text{ grad } x_1 + D^T x_1 x_2 \text{ grad } T = 0 \quad (86)$$

yields the ratio

$$\frac{D^T}{D_{12}} = - \frac{\text{grad } x_1}{x_1 x_2 \text{ grad } T} \quad (87)$$

known as the Soret coefficient, from which follow by definition the dimensionless quantities

$$k_T = x_1 x_2 \frac{D^T}{D_{12}} T = - \frac{\text{grad } x_1}{\text{grad } \ln T} \quad (88)$$

and

$$\alpha_T = \frac{D^T}{D_{12}} T = - \frac{1}{x_1 x_2} \frac{\text{grad } x_1}{\text{grad } \ln T} \quad (89)$$

This equation may be readily integrated if α_T is assumed independent of composition and temperature, an assumption which is reasonably justifiable for the former but may not be very good for the latter

$$\int_{\Delta T} \frac{\text{grad } x_1}{x_1 (1-x_1)} = - \alpha_T \int_{T_H}^{T_C} \text{grad } \ln T \quad (90)$$

which, after integrating by parts, yield

$$\alpha_T = \ln q / \ln (T_H / T_C) \quad (91)$$

where

$$q = \left[x_1 / (1-x_1) \right]_{T_H} / \left[x_1 / (1-x_1) \right]_{T_C} \quad (92)$$

The quantity q is known as the separation factor.

Equations (91) and (92) are the working equations for determining the thermal diffusion factor from the experimental conditions.

In each of the four experimental methods described in the following, the apparatus configuration is different and additional theory pertinent to the dynamics or material balance of the components in the device is necessary to extract the desired result.

One final and rather complicated expression remains to be presented here. That is the theoretical expression obtained from the rigorous kinetic theory which expresses the thermal diffusion factor in terms of the two-particle interactions, or intermolecular potential. This is most readily expressed in Chapman's determinant notation,

$$\alpha_T = \lim_{m \rightarrow \infty} \left(x_1 x_2 A_{00}^{(m)} \right)^{-1} \left\{ x_1 A_{01}^{(m)} \left[(M_1 + M_2) / 2M_1 \right]^{1/2} + x_2 A_{0-1}^{(m)} \left[(M_1 + M_2) / 2M_2 \right]^{1/2} \right\} \quad (93)$$

The quantities $A_{ij}^{(m)}$ are determinants obtained from a master determinant $A^{(m)}$ of order $2m + 1$ by striking out columns i and j . As usual, the subscript 1 refers to the heavier component, x is the mole fraction, and M is the respective molecular weight. The order of approximation to α_T is m and the first three approximations, which are those usually encountered, are designated $[\alpha_T]_1$, $[\alpha_T]_2$, and $[\alpha_T]_3$. The elements of $A^{(m)}$, which have been obtained for up to third order by Mason [71], are complicated functions of the collision integrals, molecular diameters, and molecular weights. The explicit expressions are too lengthy to be presented here.

It is this expression that would be used to test a particular intermolecular potential against experimental measurements.

1.2.1 The Two-Bulb Method

The first experimental confirmation of thermal diffusion in gases was obtained using the two-bulb method by Chapman and Dootson [70], as mentioned previously. They simply connected two bulbs together with a tube, filled the apparatus with an approximately equimolar mixture of H_2/CO_2 or H_2/SO_2 and heated one bulb. They found the hydrogen to be slightly enriched in the hot bulb by about 2 to 3% over that in the cold bulb. The concept of the two-bulb experiment is shown in Figure 13 using as an example the apparatus of Ibbs [72]. The method is very straightforward but one must orient the apparatus vertically with the hot bulb on top to

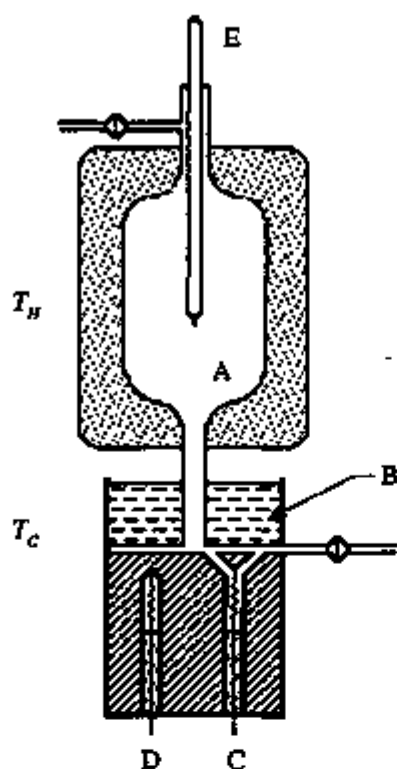


Figure 13 - Two-bulb apparatus used by Ibbs [72] for measuring binary gas separations "in situ" at average temperatures above ambient. A) Glass vessel surrounded by a heating jacket and held at temperature, T_H ; B) water bath held at temperature, T_C ; C) katharometer for measuring gas composition in cold bulb; D) reference gas for katharometer; and E) thermometer for measuring T_H .

avoid convection in the connecting tube. Also the bulbs and connecting tube must be sized in such a fashion that the equilibrium time is not excessively long. Because the separations are very small for a single stage separation, the method of analysis becomes an important consideration in the experiment. Early workers [70, 72] used a katharometer mounted in one of the bulbs which measured the change in composition of the mixture through the thermal conductivity variation which is a function of composition. The change in composition in the bulb containing the katharometer can be enhanced by making its volume smaller than the other bulb. A modern variation is to use a small solid state sensor called a thermistor to measure the mixture composition [73]. The thermistor is particularly useful at low to intermediate temperatures because various types are available with large negative coefficients of resistance for a given temperature range.

A second method of analysis which is inherently extremely sensitive, is counting disintegrations from a radioactive tracer. Several workers [74, 75], have used this technique but the method is generally restricted to trace amounts of the radioactive component for practical reasons. A third popular method is to remove a sample from the experiment and analyze it in a mass spectrometer. This method has the advantage, or at least potential, for excellent absolute accuracy for most gases and isotopic mixtures, but it is "invasive" in the sense that taking the necessary samples may disrupt the process substantially so that sampling is normally done at the end of the experiment. The first two methods are non-destructive in that they do not disrupt the course of the experiment.

In the case of the two-bulb apparatus, one region is held at a fixed temperature and the temperature of the other region is varied. From a series of experiments, α_T is obtained from the slope of the logarithmic plot of T_H/T_C vs. the separation factor. The drawback of this method is that the numerical value of α_T is very sensitive to the derivative of the curve of unspecified functional form which must be fitted to the experimental points, each of which in turn has uncertainties in $\ln q$ and $\ln (T_H/T_C)$ associated with it. The problem is particularly severe at the end points of the curve. The apparatus shown in Figure 13 depicts the case where the lower temperature, T_C , is held constant by the water bath B and gas in the upper bulb A is raised to various higher temperatures by the heating mantle around A.

Conversely the apparatus may be constructed in such a manner that the upper reservoir is held at a constant temperature and the lower reservoir is varied to successively lower temperatures. An example of such an apparatus is that of Ghozlan and Los [75] shown in Figure 14 which was used for the determination of α_T for the hydrogen isotopes (including tritium). The upper chamber contained an ionization chamber to determine the concentration of tritium in the mixture.

The apparatus constructed by Weissman [76] and extensively modified by Taylor [77] for use down to very low temperatures ($\sim 2\text{K}$) on the helium isotopes, is shown in Figure 15. Because it is generally impractical to have a valve in the low temperature region which isolates the cold reservoir, it is necessary to obtain the composition at T_C from the feed and hot reservoir compositions. A rigorous theory for the two-bulb experiment was derived by Lonsdale and Mason [74, 78] for the case of one component present only in trace quantities based on a mass balance in the hot and cold reservoirs and the connecting tube. Taylor [77] extended the theory to the general binary mixture case. Now let X represent either one of the compositions C_1 or C_2 of the binary mixture, expressed as mole fraction. When the feed composition, $x_F \equiv x_H(0) \equiv x_C(0)$, and the steady state hot bulb composition, $x_H(\infty)$, are known, the composition in the cold bulb at the end of the experiment with a connecting tube of length L is

$$x_C(\infty) = x_F + \frac{V_H T_C}{V_C T_H} \left[x_F - x_H(\infty) \right] - \frac{\Delta n_L}{N_C} \quad (94)$$

where Δn_L is the change in the number density of the light component in the connecting tube during the experiment and N_C is the total molecular density in the cold bulb which remains constant during the course of the experiment.

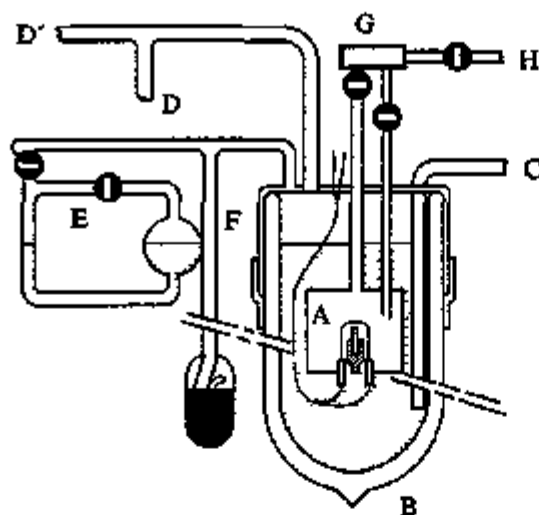
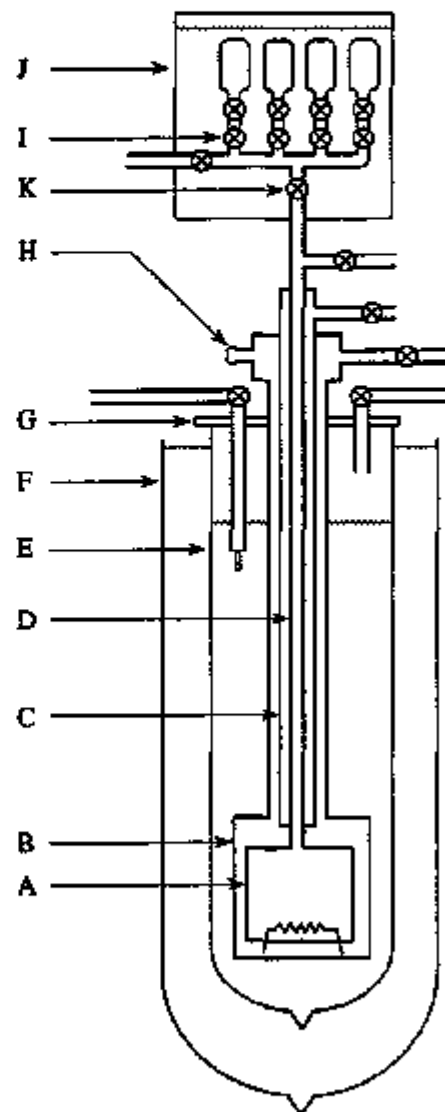


Figure 14—Two-bulb apparatus used by Ghozlan and Los [75] for determining α_T at low temperatures. A) Lower reservoir held at temperature, T_C ; B) Dewar vessel containing cryogenic fluid; C) tube for introducing coolant; D) coolant vapor vent; D') vacuum line for pumping on coolant; E) manometric device for coarse control of coolant vapor pressure; F) manometric device for fine control of vapor pressure; G) upper reservoir held at temperature, T_H ; and H) gas inlet line

Figure 15—Schematic of the two-bulb device used by Taylor [77] to measure thermal diffusion factors on helium isotopes down to 2K. The components are: A) lower chamber containing three different temperature sensors, one Pt resistor mounted in the gas, another embedded in the copper base along with an Allen-Bradley carbon resistor; B) vacuum/exchange gas region; C) vacuum jacket around connecting tube; D) connecting tube; E) inner Dewar for LHe; F) outer Dewar for LN₂; G) supporting flange; H) vacuum pass through for sensors, J) manifold for four sample bottles; J) water bath controlled by Haake circulator; and K) isolation valve.



The term $\Delta n_L/N_C$ is the correction for the finite volume of the connecting tube and is determined by the following:

$$\begin{aligned}\Delta n_L &= n_L(\infty) = \int_0^L dn_L(\infty, z) - N_L x_F \\ &= \int_0^L x_L(\infty, z) dN_L(z) - x_F \int_0^L dN_L(z)\end{aligned}\quad (95)$$

The differential $dn_L(\infty, z)$ represents the composition gradient at the steady state due to the temperature gradient along the connecting tube. The variable z stands for any point on the connecting tube. Since $A dz = dv$, the quantity N_L can be evaluated in terms of the ideal gas law for an incremental volume.

$$\Delta n_L = \int_0^L \frac{x(\infty, z) P N_o A}{RT(z)} dz - x_F \int_0^L \frac{P N_o A}{RT(z)} dz \quad (96)$$

In order to integrate this equation, expressions must be assumed for the temperature and composition distributions. A reasonable approximation for the temperature distribution is

$$T(z) = T_H - \left(\frac{T_H - T_C}{L} \right) z \quad (97)$$

and, from Equations (91) and (92) by letting $X_L(\infty, z) = X_C(\infty, z)$, for the composition distribution

$$x_L(\infty, z) = \left[1 + \left(\frac{1}{x_H(\infty)} - 1 \right) \left(\frac{T_H}{T(z)} \right)^{\bar{\alpha}_T} \right]^{-1} \quad (98)$$

The assumption is made here that $\bar{\alpha}_T$ is an "effective" thermal diffusion factor which must be obtained iteratively. Substitution of Equations (97) and (98) into (96) yields an expression which can be analytically integrated by making the change of variable $x = a + bz$. The second

term can be integrated directly. After integration and simplification, and noting that $AL = V_T$, the correction term is

$$\frac{\Delta n_L}{N_C} = \frac{V_T T_C}{V_C (T_H - T_C)} \ln \left\{ \left(\frac{T_H}{T_C} \right)^{1-x_p} \left[x_{H(\infty)} + \left[1 - x_{H(\infty)} \right] \left(\frac{T_H}{T_C} \right)^{\bar{\alpha}_T} \right]^{-1/\bar{\alpha}_T} \right\} \quad (99)$$

The cold reservoir composition, $x_{C(\infty)}$, can now be calculated from the experimental conditions and apparatus dimensions. The separation factor, q , and the thermal diffusion factor, α_T , for the experiment may be calculated from Equations (91) and (92) respectively. The value of α_T obtained must, of course, agree with the "effective" value of $\bar{\alpha}_T$ used in evaluating the correction factor. If it does not, the calculation must be iterated until a consistent value is obtained.

Taylor [77] has compared the "slope" method to the iterative procedure above for the determination of α_T for the helium isotopes. The problem in the second method is that a specific value of the temperature cannot be assigned to α_T , whereas in the "slope" method it can. Taylor found, however, that where most of the gas in the experiment was at a temperature at or near T_C and α_T did not vary too rapidly with temperature in the region of interest, the iterative procedure gave more reasonable results. Apparently the inaccuracy introduced by differentiating the logarithmic plot of T_H/T_C vs. q , along with the inherent experimental uncertainty in the data, introduced a somewhat spurious temperature dependence in α_T which was not exhibited by the iterated value of $\alpha_T(T_C)$.

Quite a few investigators have built and operated two-bulb experiments in addition to those already mentioned. An incomplete list would include, but not be limited to, the group at Exeter, U.K., under Grew [79], de Vries and coworkers at FOM-Institute in Amsterdam [80] and, more recently, Dunlop's group [81, 82] in Adelaide, Australia. These citations show the experimental apparatus and discuss operating procedures. The accuracy of the two-bulb will depend strongly on the analytical technique used to measure the composition because the separation is usually very small with this method. In addition, differentiation of the separation curve magnifies scatter and may introduce an undetectable bias. Barring this, one might reasonably expect accuracies of approximately ± 5 to 8%, depending on the binary mixture. Dunlop's group reports an accuracy of approximately 2 to 3%, but in a very limited temperature range.

1.2.2 The Trennschaukel (Swing Separator)

A device which has proven quite useful in the experimental determination of the thermal diffusion factor was developed by Clusius and Huber [83]. In principle, the trennschaukel, or swing separator, is a number, n , of two-bulb experiments connected in series as shown in Figure 16. The top and bottom ends of the tubes (approximately $1/3$) are embedded in isothermal regions held at temperatures T_H and T_C , respectively. The temperature gradient, ΔT , is established in the middle portion of the tubes. By connecting each successive tube top to bottom with a capillary and gently moving the gas to and fro by means of a pump, the concentrations of the components of the gas mixture in the top of one tube are made essentially identical with those at the bottom of the next tube. Since the temperature gradient is applied in the vertical direction with the hot end at the top, the effect of convection is eliminated. The separation factors of the individual tubes are multiplicative, so an n -fold increase in the separation is realized. Because n may be ten or twenty, an order of magnitude increase is quite feasible, resulting in a considerable analytical advantage over the two-bulb method. As simple as the apparatus in Figure 16 appears, it is still subject to certain restrictions which, if violated, will invalidate the results. For example, one must operate sufficiently long so that steady state concentrations in the regions under and over the pump are approached. The frequency of pumping lies within certain limits. If one pumps very slowly, backward diffusion in the capillaries sets in, but if pumping is too rapid, the motion of the gas disturbs the thermal diffusion balance in the tubes. The theory of material transport in the device was derived by van der Waerden [84] and yields explicit expressions involving the physical characteristics and operating parameters which must be considered in order to ensure successful operation.

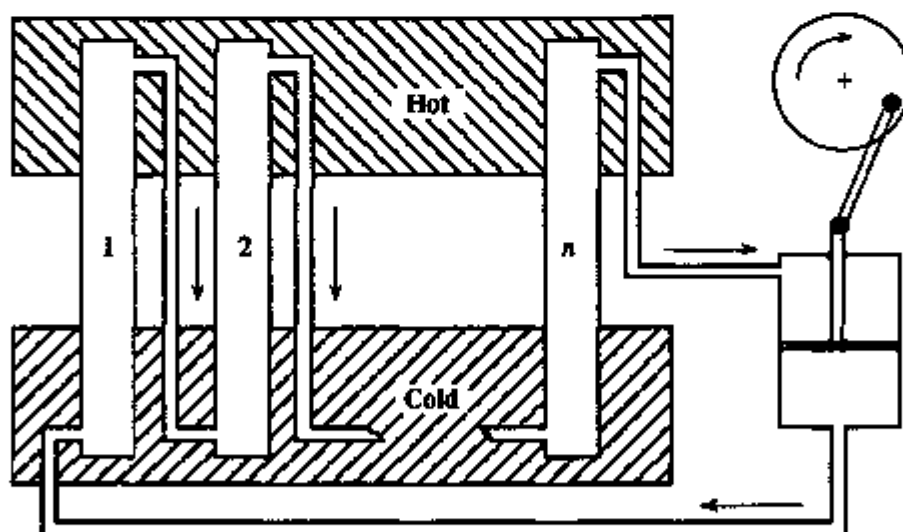


Figure 16 - Principle of the trennschaukel or "swing separator". A given number of tube/capillary pairs are connected top-to-bottom and the contained gas mixture is swung to-and-fro by a pump. A temperature difference, $\Delta T = T_H - T_C$, is imposed across the n tubes by embedding the top approximately $1/3$ of the tubes in an isothermal region at T_H and the bottom $1/3$ in another isothermal region at T_C .

A practical limit will be encountered in the number of tube/capillary pairs employed by virtue of viscous flow restrictions encountered in the capillaries (Poiseuille's Law). A pressure gradient will be established in the capillaries due to pumping and this will in turn decrease the quantity of gas that is transported forward from tube to tube. The effect will be greatest in the middle tubes and will not only limit the total number of stages but will also restrict the operating conditions. Utilizing Poiseuille's Law, the pressure drop in the capillaries is equated to the volumetric rate of transport to yield a set of n time-dependent differential equations whose solutions are complex exponentials having both an amplitude and phase component. If the amplitude, a , represents the pumped volume per half cycle, then the maximum compression is realized in the middle tube with

$$a' = af = a \left[1 - \frac{1}{192} \left(\frac{nV}{cP_0} \frac{2\pi n}{t_p} \right)^2 \right] \quad (100)$$

where V is the tube volume, P_0 is the gas pressure, and t_p is the pump period. The quantity c derives from the Poiseuille equation, e.g.,

$$c = \frac{\pi d^4}{128 \eta_T l} \times 0.13332 \times 10^4 \quad (101)$$

with the capillary diameter, d , and length, l , in centimeters and the viscosity, η_T , in poise at temperature T . If the volume on each side of the pump were exactly equal to the tube volume, then n could be replaced by $n + 2$ and an exact solution would result. Where the pump holdup is a fraction, e' , between 0 and 1 of the tube volume, a good approximation is just to replace n in Eq. (28) with $n + 2e'$.

It is of course possible to design a trennschaukel and/or operate it in such a manner that the multiplicative factor, f , approaches zero and no transport at all takes place in the middle tubes, or a phase reversal results. van der Waerden has suggested that conditions be such that $f \sim 0.95$ so that the diminution in the amplitude can be neglected.

The following three corrections for trennschaukel operations are applied to the measured composition difference at the end of the experiment. Equation (92) must therefore be rewritten in terms of this difference, e.g.,

$$Q = \frac{1 + \left[\Delta x_1(\text{corr}) / x_1(T_C) \right]}{1 + \left[\Delta x_2(\text{corr}) / x_2(T_C) \right]} \quad (102)$$

where Q is the separation factor for the trennschaukel across n tubes and

$$\Delta x_1(\text{corr}) = \left[x_1(T_H) - x_1(T_C) \right]_{\text{meas}} / \left[(1 + \zeta) \delta \varepsilon \right]. \quad (103)$$

A similar expression holds for $\Delta x_2(\text{corr})$ where $x_2 = 1 - x_1$. The elementary separation factor is $q = Q/n$.

i) Approach to equilibrium, δ :

The equations for the approach to equilibrium are derived from a concentration balance in the n tubes and the pump volumes. The solution of the $n + 2$ differential equations is an exponential with a superimposed sine wave due to pumping. Since equilibrium is approached exponentially, it is reasonable to define an operating half-life for the experiment and operate for a sufficient number of half-lives so that equilibrium is closely approached. The expression for the half-life is

$$t_{1/2} = \left(t_p V / 2a + L^2 / D_{12} \right) \left[(n + 1) / \pi \right]^2 \ln 2 \quad (104)$$

where L is the tube length and D_{12} is the binary mixture diffusion coefficient at the pressure and average temperature of the experiment.

The equilibrium half-life is calculated from the operating conditions and the correction factor

$$\delta = \left(1 - [1/2]^N \right) \quad (105)$$

(where N is the number of half-lives) is applied to the measured concentration difference.

ii) Back diffusion in the capillaries, ε :

The major transport of either species due to thermal diffusion takes place in the tubes, whose cross section is large compared to that of the capillaries. There is, however, a finite amount of material transported back through the capillaries which tends to decrease the measured separation. A general transport equation for material through either the tubes or capillaries is obtained by setting the rate of change of the composition over the volume of a tube

or capillary equal to the sum of the molecular flux from Equation (86) plus the material transported by the pump. Thus

$$A \frac{d}{dt} \int_0^z K dz = a \omega \sin \omega t [K]_0^z - AD_{12} [C_z - K_z]_0^z \quad (106)$$

where A is either the cross section of a tube or capillary, ω is the pumping frequency, a is the pumped volume, K is the composition at time t , C is the equilibrium composition and C_z , K_z are the spatial derivatives of C and K .

Solution of this transport equation for the capillaries yields the correction factor

$$\varepsilon = 1 - \left(\pi d t_p D_{12} / 8 a l \right) \quad (107)$$

with the variables as defined previously.

iii) Disturbance due to pumping, ζ :

The final correction term is unusual in that it leads to an increase in the value of α_T and was first predicted theoretically rather than first being observed experimentally. It is obtained by solving the general transport equation in the tubes with simultaneous thermal diffusion and transport due to pumping. The solution of the equation is quite lengthy and leads to a correction term, ζ , which is conveniently expressed in terms of hyperbolic functions,

$$\zeta = \frac{a \pi}{2V} \operatorname{Im} \left[- \frac{\sinh \gamma (1 - 2s)}{(1 - 2s) \sinh \gamma} \right] \quad (108)$$

with

$$\gamma = 1/2 \left(l^2 \omega / 2D_{12} \right)^{1/2} (1 + i) \quad (109)$$

and s the fraction of the total tube length in each of the isothermal zones.

The experimental thermal diffusion factor is obtained from Equation (91) using the overall separation factor, Q , divided by the number of stages in the trennschaukel. Note that all of the apparatus dimensions and operating parameters appear only in the correction terms δ , ε , ζ which are applied to the measured composition difference at each end of the device. Equation (91) is now

$$\alpha_T = \frac{1}{n} \frac{\ln Q}{\ln (T_H / T_C)} \quad (110)$$

where n is the number of tube/capillary stages in the experimental device.

One example of a trennschaukel system, which was constructed by Taylor et. al. [85], is shown in Figure 17 and has been in operation for quite a few years. The device contains twenty Inconel tube/capillary pairs welded into two massive toroidal nickel blocks. The gas is swing to-and-fro by a welded metal bellows pump mounted on the top block and the entire apparatus is mounted in an environmental chamber. The bottom block, which is heavily insulated, contains passages through which either compressed air or cold LN_2 vapors are circulated by means of a surrounding manifold. The system can be operated in a temperature range from approximately 200 to 1000K. Samples are analyzed by mass spectrometric analysis.

A trennschaukel designed for low temperature operation is shown in Figure 18 [86]. This particular device has ten tubes in a circular configuration and is placed inside a cryostat. Both top and bottom blocks are wound with heater wire and instrumented with platinum and carbon resistors for temperature measurement and control. The support for the entire apparatus inside the cryostat is a Cryotip[®] refrigerator passing through the toroidal top block and attached to the lower block. The temperature differential may then be established in either of two ways: 1) a cryogenic fluid (LHe , LNe , LN_2 , etc.) is filled well up the bottom block and it's temperature is

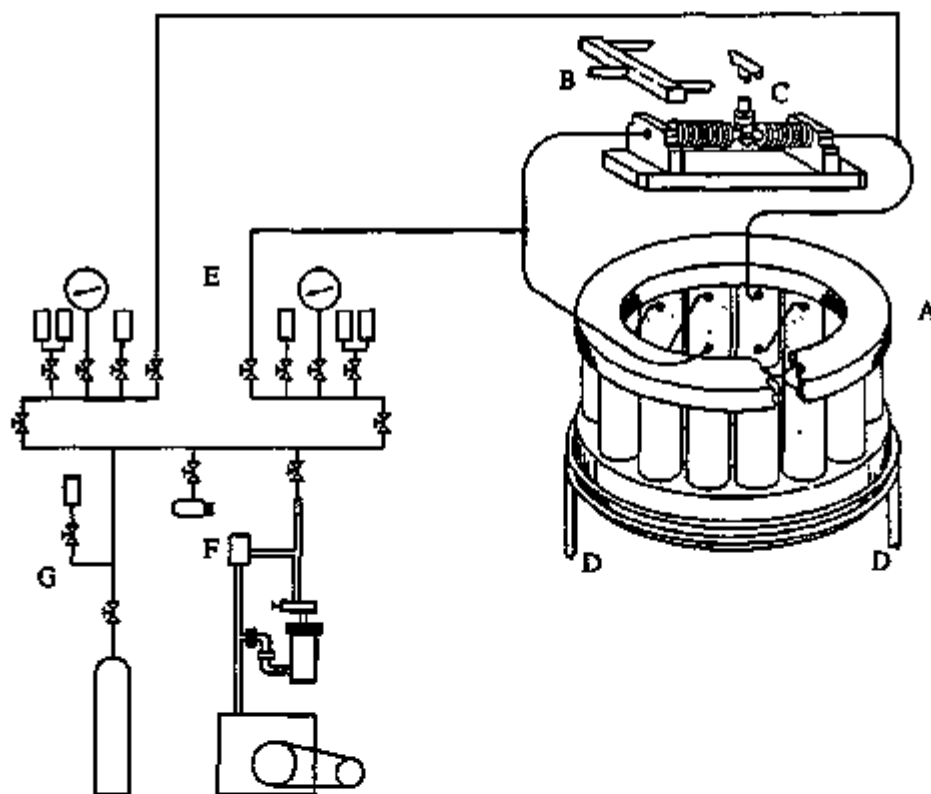


Figure 17 – High temperature nickel/inconel trennschaukel used by Taylor et. al. [85] to measure α_T for numerous gas mixtures in the temperature range 200 to 1000K. A) 20-tube device with massive nickel blocks connected by inconel tubes and capillaries; B) drive shaft to pump mechanism; C) bellows pump; D) lower block cooling manifold; E) sampling parts; F) vacuum system; and G) feed gas supply.

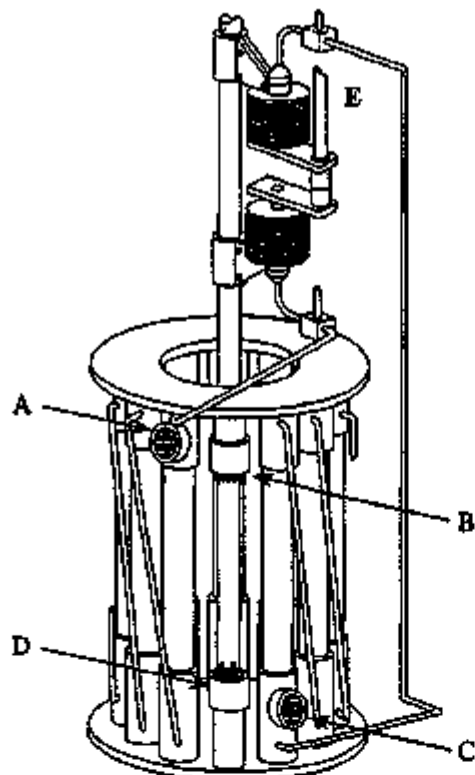


Figure 18 - Low temperature 10-tube trennschaukel [86] instrumented with thermistors for "in-situ" measurement of the separation. The components are: A) sensor for unknown composition at T_H ; B) sensor in reference gas at T_H ; C) sensor for unknown composition at T_C ; D) sensor in reference gas at T_C ; and E) bellows pump that swings gas.

regulated by means of the vapor pressure of the liquid, or 2) the bottom block is cooled by Joule-Thomson expansion in the Cryotip[®] refrigerator. In either case ΔT is established by heating the top block. The compositions in this device may be sampled "in situ" by strategically placed thermistors or by samples withdrawn for mass spectrographic analysis. The temperature range accessible is approximately 2 to 250K.

As was the case with the two-bulb method, the accuracy with which α_T may be determined is affected by the binary gas mixture being investigated and, consequently, the analytical method utilized to determine the separation. The number of tubes employed helps this and under most circumstances an accuracy of approximately ± 5 to 7% should be attainable. Exception to this would be measurements made at extreme temperature where temperature control and uniformity is difficult, or when the mass difference of the components is quite small.

A number of other groups have employed "swing separators" in thermal diffusion research. Among these are Watson and coworkers [87-89] at Yale University, Kistemaker's group [90-93] at FOM-Institute, and researchers at the Gulbenkian Institute in Lisbon [94]. Oost and Haring [95] proposed an interesting variation of the trennschaukel which utilizes the thermo-syphon effect to transport material from one tube to the next instead of pumping to and fro. The method eliminates some of the transport corrections discussed above but apparently complicates the experimental apparatus considerably. Illustrations of the experimental equipment are given in the references.

1.2.3 The Thermal Diffusion Column

A third experimental method which may be employed to measure thermal diffusion factors is the "trennrohr" or thermal diffusion column, the invention of which is attributed to Clusius and Dickel [96]. After the initial discovery of the thermal diffusion effect, little progress was made on the application of a temperature gradient to practical separations of gas mixtures, for example rare isotopes, because early workers quickly recognized that a single stage separation was very small, even for large temperature differences. Shortly before World War II Clusius and Dickel discovered that the thermal diffusion separation could be enhanced tremendously by hanging a hot wire in a tall, thin vertical column and using the natural convection currents set up to sweep the light component at the hot wire up the column and the heavy component at the cold wall down.

A rigorous mathematical treatment of the hot wire column is a formidable task and does not readily yield to a solution unless simplifying assumptions are made. Furry, Jones and Onsager [97] first treated mathematically the hydrodynamical problem of convection between plane-parallel walls, then Furry and Jones [98] extended the theory to the cylindrical case. A review article by Jones and Furry [99] nicely summarized the development of column theory immediately following World War II.

The behavior of the column is based on the hydrodynamic equation representing the convection current set up between the hot and cold walls. The gas mixture rises at the hot wall and descends along the cold wall approximately as shown in Figure 19. The effect of thermal diffusion is to preferentially drive the lighter molecules to the hot region where they enter the rising convection current. The lighter molecules are carried upward and the heavier ones are carried downward so that a concentration gradient is established in the vertical direction. The "unmixing" is opposed by ordinary diffusion and by convection which tend to neutralize any separation along the column. The steady state concentration gradient is expressible as a partial differential equation in two variables (radial and axial coordinates) whose explicit form results from the driving force of thermal diffusion and the remixing effects of ordinary diffusion and convection. The FJO theory [97] considerably simplified the computational problems by decoupling the transverse and axial parts of the transport by means of an assumption regarding the radial composition distribution. FJO assumed the change of composition in the radial direction is small so that except when multiplied by the convective flow rate, the composition is a constant across the annulus. The FJO theory was developed during World War II and was specifically derived to describe column behavior for the separation of heavy isotopes, namely $^{235}\text{UF}_6/^{238}\text{UF}_6$.

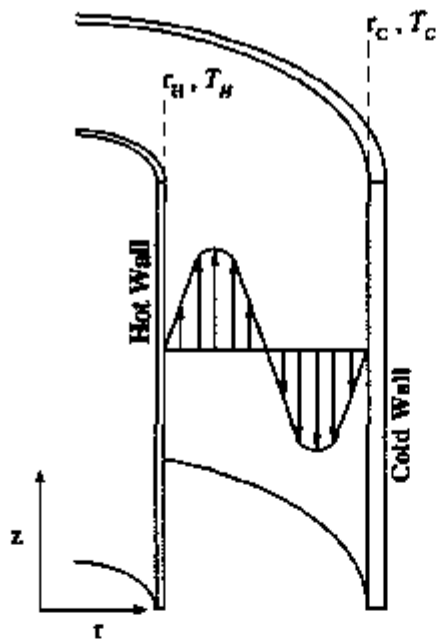


Figure 19 - The form of the convection currents between the hot and cold walls of the separation column. The symmetrical form indicated by the arrows is only approximate; for large differences in the radii and/or temperature difference, the curve becomes significantly asymmetric.

More recently Rutherford [100] has extended the previous theory to light isotopes by changing the reference frame of the flux equation to the center-of-mass system and writing the transport equation below in terms of the mass fraction. He reports the transport, τ_1 , to be:

$$\tau_1 = Hw_1(1 - w_1) - (K_c + K_d)\left(dw_1/dz\right); \quad (111)$$

with, respectively, the initial transport coefficient

$$H = 2\pi \int_{T_c}^{T_H} \left[\alpha_T G(T)/T \right] dT; \quad (112)$$

the convective remixing coefficient

$$K_c = \left(2\pi/Q\right) \int_{T_c}^{T_H} \left[\kappa G^2(T) D_{12} \rho \right] dT; \quad (113)$$

and the diffusive remixing coefficient

$$K_d = \left(2\pi/Q\right) \int_{T_c}^{T_H} \kappa D_{12} \rho r^2 dT. \quad (114)$$

Here T_c and T_H are the cold and hot wall temperatures, α_T is the thermal diffusion factor, $2\pi Q$ is the radial heat flow per unit length per second, κ is the thermal conductivity, D_{12} the diffusion coefficient, ρ the density, and r is the radial coordinate.

The quantity $G(T)$ is related to the mass circulation rate in the column and is given by solution of the fourth order differential equation

$$Q^3 \frac{d}{dT} \frac{1}{r^2 \kappa} \frac{d}{dT} \frac{\eta d}{\kappa dT} \frac{1}{\rho \kappa r^2} \frac{dG}{dT} = -g \frac{d\rho}{dT} \quad (115)$$

where g is the acceleration of gravity and η is the viscosity. The boundary conditions require that G and dG/dT are zero at the walls. It should be noted that use has been made of the relation

$$\ln(r/r_c) = -\frac{1}{Q} \int_{T_c}^T \kappa dT \quad (116)$$

which transforms the radial coordinate to temperature.

The theory of the T.D. column is complicated and to extract α_T from column measurements requires a carefully constructed column as well as knowledge of certain physical properties, e.g. the thermal conductivity, viscosity, mass diffusion coefficient and gas density of the mixture. The early workers recognized these difficulties and generally utilized the column method when its large separatory power was required as in the case of isobaric mixtures or isotopes where the mass difference was very small. Relative measurements were made by utilizing a thermal diffusion factor obtained from some other source and evaluating column performance at the maximum of the separation curve. Other mixtures were then introduced into the column and the relative separation at the maximum obtained. Two notable examples of this method were the work of Schirdewahn et. al. [101] on the hydrogen isotopes and de Vries and Haring [102] on isotopically substituted carbon monoxide. The apparatus of Schirdewahn et. al. is shown in Figure 20. Both groups used glass columns with hot wires, however de Vries and Haring achieved additional separation by connecting three columns in series and swinging them in trenschaukel fashion.

Other groups that have utilized the column method for determining α_T are Raman et. al. [103, 104], Kirch and Schütte [105] on isotopic UF_6 , and Savirón and coworkers [106-108] who studied unlike and isotopic mixtures of the noble gases.

Rutherford [109] has constructed a precision thermal diffusion column and developed a method for measuring absolute values of α_T from the column, a diagram of which is shown in Figure 21. He has found that the theory of the thermal diffusion column is much more accurate than previously supposed and has suggested that previous discrepancies between experiment and theory were due to imprecise knowledge of the column geometry and operating conditions and the use of inaccurate values of the gas properties in the theoretical expressions. His method is to make static separation measurements (net mass flow = 0) in the column as a function of pressure. In an earlier paper [110] he had shown that accurate values of the initial transport coefficient could be obtained under static conditions by using the pressure-independent diffusive remixing coefficient, K_d , calculated from theory. This requires, of

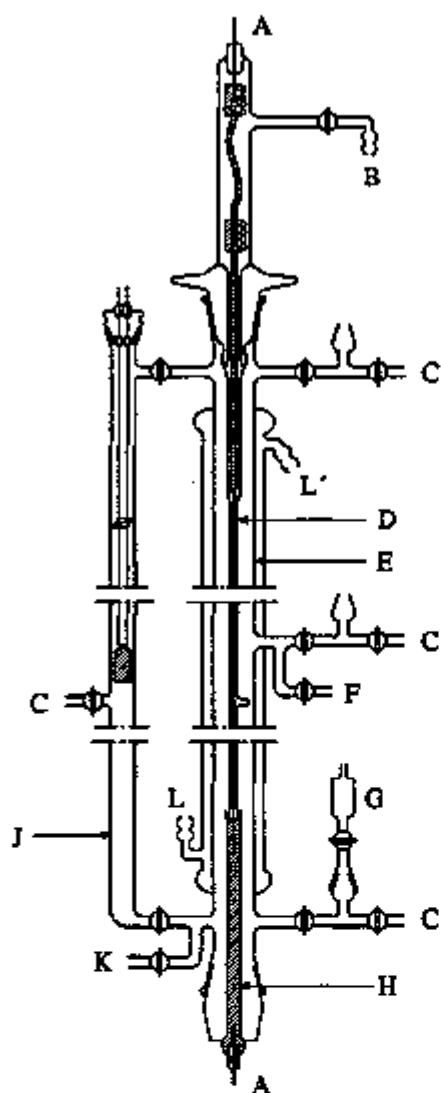


Figure 20 - Thermal diffusion column used by Schirdewahn et. al. [101] for determining α_T in hydrogen isotope mixtures. The components are: A) tungsten wire; B) vacuum and hydrogen; C) vacuum; D) hot wire; E) outer wall of column; F) gas inlet; G) ampoule; H) mercury bath; J) convective circuit; K) connection to mercury manometer; and L, L') inlet and outlet of the cooling water.

course, that reliable values of D_{12} are available, or can be calculated from kinetic theory. Rutherford writes Equations (112) and (113) in reduced form, e.g.,

$$H' = \left(2\pi/p^2Q^3 \right) \int_{T_H}^{T_C} \frac{\alpha_T G(T)}{T} dT = \bar{\alpha}_T \xi \quad (117)$$

where ξ is defined by

$$\xi = \frac{2\pi}{p^2Q^3} \int_{T_H}^{T_C} \frac{G(T)}{T} dT. \quad (118)$$

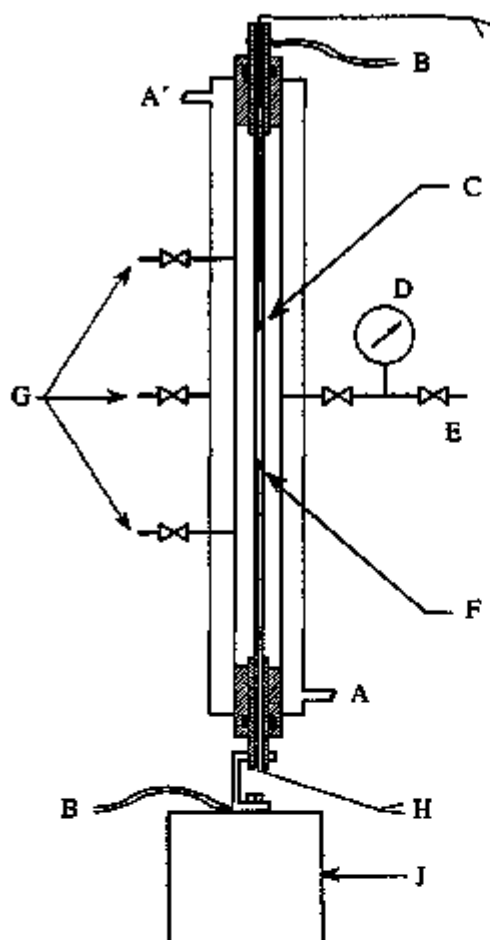


Figure 21 - Precision thermal diffusion column built by Rutherford [109] for measuring absolute values of α_T . The components are: A, A') water inlet and outlet; B) electrical leads; C) thermocouple; D) precision dial manometer; E) gas supply; F) resistance thermometer; G) sample ports; H) to hot wall temperature controller; and J) weight.

In Equation (117) $\bar{\alpha}_T$ is the mean thermal diffusion factor between T_H and T_C and

$$K'_C = \left(2\pi/p^4 Q \right) \int_{T_H}^{T_C} \left[\kappa G^2(T) D_{12} \rho \right] dT \quad (119)$$

Under static conditions Equation (111) then becomes

$$H' p^2 w_1 w_2 - \left(K'_C p^4 + K_d \right) dw_1/dz = 0 \quad (120)$$

The solution of Equation (120) is

$$\ln q/L = \frac{\left(H'/K_d \right) p^2}{\left(K'_C/K_d \right) p^4 + 1} \quad (121)$$

where L is the length of the column and q is the separation factor defined by

$$Q = \left[\frac{w_1}{w_2} \right]_{z=L} / \left[\frac{w_1}{w_2} \right]_{z=0} \quad (122)$$

Now the ratios $(H'/K_d)_{exp}$ and $(K'_z/K_d)_{exp}$ are determined by a nonlinear least squares fit to Equation (121) where $\ln q/L$ has been determined as a function of pressure. Recognizing that

$$H' = \left[\frac{H'}{K_d} \right]_{exp} / \left[K_d \right]_{theo} \quad (123)$$

the numerical value of $\bar{\alpha}_T$ is obtained from Equation (117) by evaluating ξ theoretically. Rutherford then checks his column performance by comparing the experimental value of K'_z/K_d to the corresponding theoretical value. Because both K'_z and K_d are independent of $\bar{\alpha}_T$, this comparison should provide a good check of column operation. It should also be noted that in using this method, T_c and T_H should not be too far apart, so that a reasonably accurate average temperature can be assigned to the mean value, $\bar{\alpha}_T$. Results obtained by this method were found to be in excellent agreement with measurements made in a swing separator [85]. The separation power of thermal column minimizes the analytical problem, however, one must have an accurate knowledge of the other transport properties. Rutherford [100] reports an uncertainty of $\pm 9\%$ for helium isotopes (properties well known) and expects an accuracy of approximately 10 to 15% for heavier systems.

1.2.4 The Dufour Effect

At the beginning of this report the equivalence of the coefficient of thermal diffusion, D^T , to that of the Dufour coefficient, D^D , was shown through use of the Onsager reciprocal relation, Equations (34) and (35). Because of this equivalence it is possible to experimentally determine the thermal diffusion factor by measuring the temperature difference produced by the mixing of two gases. In a classic piece of work, Waldmann [111] constructed the apparatus shown in Figure 22 in which he determined α_T for nine pairs of gases. He was even able to observe the inverse temperature effect with Ar/CO₂ in which α_T decreases with increasing temperature.

The cell consisted of a metal cylinder with two holes approximately 0.75 cm diameter bored side-by-side down the length of the cylinder. A slide, s , with tightly stretched mesh, N , was slipped longitudinally down the cylinder separating the two holes to provide the diffusion path. Temperatures were measured by the change in resistance of extremely fine gold wires whose resistance was proportional to the gas temperature over the range 20 to 373K. By means of a Wheatstone bridge and galvanometer and, after calibration at a number of fixed points,

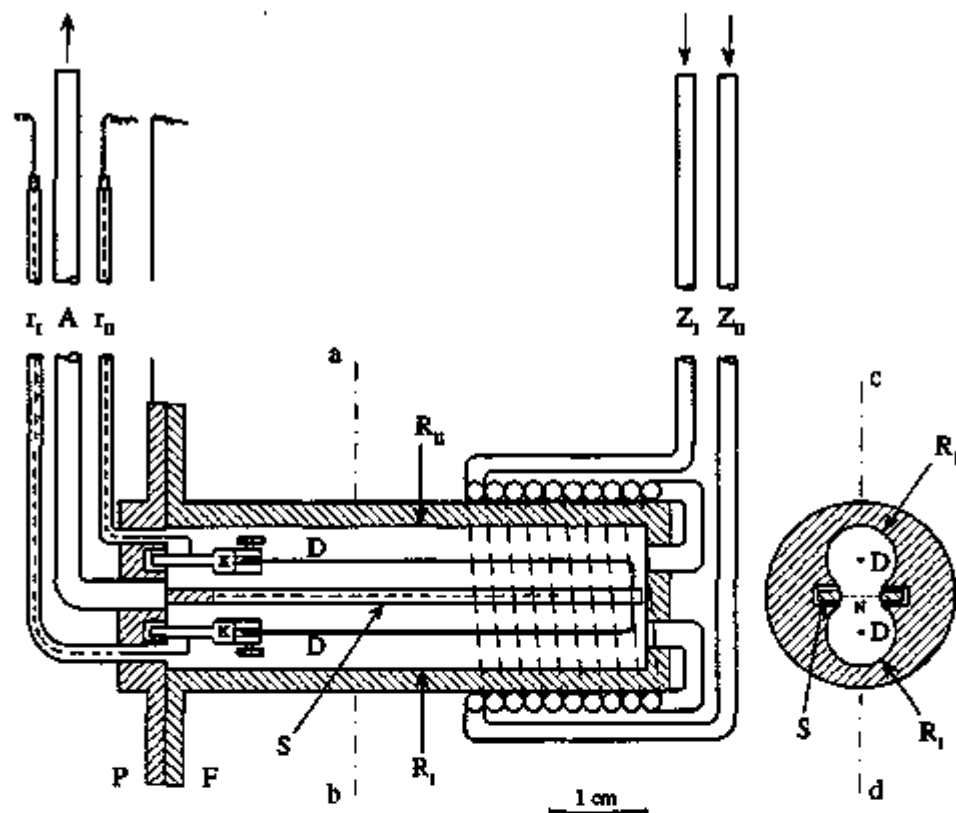


Figure 22 – Cross sections of the Dufour cell constructed by Waldmann [101]. The cross section through a-b is shown in the right hand view and that through c-d in the left hand view. The components are: $R_{1,2}$) 0.75 cm dia. parallel tubes; $Z_{1,2}$) copper cooling coils for gas entry; A) exit line for the mixed gases; D) temperature sensing gold wires; K) clamps holding the gold wires S) slide; N) diffusion grid mounted in S); P) cylinder head mounted on flange F); and $r_{1,2}$) German silver tubes/electrical pass-throughs for the temperature sensing wires.

Waldmann was able to measure changes in the gas temperature on the order of 0.002K in each of the two gas chambers.

The experiments were conducted by flowing each gas down a tube and allowing them to diffuse together, thereby establishing a slight temperature difference between the two gold wires. The stream velocity, v , of the gas was progressively increased until a maximum was observed in the temperature in the upper tube and a corresponding minimum in the lower tube, e. g. $(T - T_0)_{\max}$ and $(T - T_0)_{\min}$ respectively, where T_0 is the initial gas temperature. The starting point for derivation of the working equations for the experiment lies in applying Enskog's general equation of change to the mass and energy, e. g.

$$\rho \frac{\partial x_i}{\partial t} + \text{div } \vec{J}_i = 0 \quad (\text{mass}) \quad (124)$$

and

$$\rho \frac{dH}{dt} - \frac{\partial p}{\partial t} + \operatorname{div} \vec{J}_q = 0 \quad (\text{energy}) \quad (125)$$

where H is the molar enthalpy. Utilizing the ideal gas law and the transport properties from the kinetic theory of dilute gases, Waldmann obtained the time dependent differential equation for the change in composition and temperature as a function of the experimental parameters and macroscopic properties. These equations are:

$$\frac{dx_1}{dt} = D_{12} \Delta x_1 \quad (126)$$

and

$$\frac{dT}{dt} = K\Delta T + \delta T_\alpha \frac{dx_1}{dt} + \delta T_B \cdot 2D_{12} \operatorname{grad}^2 x_1 \quad (127)$$

where

$$K = \kappa / n \bar{C}_p \quad (128)$$

$$\delta T_\alpha = \alpha_T RT / \bar{C}_p \quad (129)$$

$$\delta T_B = b^* RT / \bar{V} \bar{C}_p \quad (130)$$

$$b^* = B_{11}^* - 2B_{12}^* + B_{22}^* \quad (131)$$

$$B^* = B - T \frac{\partial B}{\partial T} = \sum_{i,k} B_{ik}^* x_i x_k = \sum_{i,k} \left(B_{ik} - T \frac{\partial B_{ik}}{\partial T} \right) x_i x_k \quad (132)$$

with the B_{ik} being the second virial coefficients for the pure components and their mixture, \bar{C}_p the heat capacity at constant pressure, R the gas constant, κ the thermal conductivity, and \bar{V} the molar volume at p, T .

Now Waldmann noted that the last term in Equation (127) is due to the heat of mixing and can be negligible if the pressure is sufficiently low. Furthermore the gases are introduced into

each tube with a velocity \bar{v} in the + z direction along the axis of the cylinder. Equations (126) and (127) transform to

$$\bar{v} \frac{\partial x_1}{\partial z} = D_{12} \left(\frac{\partial^2 x_1}{\partial x^2} + \frac{\partial^2 x_1}{\partial y^2} \right) \quad (133)$$

and

$$\bar{v} \frac{\partial T}{\partial z} = K \left(\frac{\partial^2 T}{\partial x^2} + \frac{\partial^2 T}{\partial y^2} \right) + \delta T_\alpha \bar{v} \frac{\partial x_1}{\partial z} \quad (134)$$

Diffusion takes place at the boundary before reaching the wires in the middle of the tubes and temperature extremes (maximum above; minimum below) are developed as a function of gas flow velocity. Upon transforming to dimensionless variables and applying the boundary conditions, Waldmann obtained the following expression relating the thermal diffusion factor to the measured temperature extreme and the other experimental parameters.

$$\overline{(T - T_0)}_{extreme} = T_0 \frac{R}{c_p} \alpha_T \left[x_1(\infty) - x_1(-\infty) \right] \bar{\theta}_{max} \left(K / D_{12} \right) \quad (135)$$

The function $\bar{\theta}_{max}$ must be determined at various values of (K / D_{12}) by means of a calibration gas. This, of course, means that Waldmann's method is a relative method. It is difficult to assign an experimental uncertainty to this method as such a determination would depend on the absolute accuracy of the properties of the calibration gas. Based on a comparison with other Ar/CO₂ data, it would appear that the method determines α_T within approximately $\pm 10\%$.

SYMBOL TABLE

A	cross sectional area of tube (or capillary) (m^2)
A_{ij}	kinetic theory determinant element (dimensionless)
a	volume pumped per half cycle (m^3) (see context)
a	dimension of diffusion cell (m)
a'	maximum compression in middle table (m^3) (see context)
B	second virial coefficient ($m^3 \text{ mol}^{-1}$)
B^*	defined by Eq. (132) ($m^3 \text{ mol}^{-1}$)
b^*	defined by Eq. (131) ($m^3 \text{ mol}^{-1}$)
C	composition (molar percentage)
C_x	spatial derivative of C (molar percentage m^{-1})
\bar{C}_p	molar heat capacity ($J \text{ mol}^{-1} \text{ K}^{-1}$)
c	Poiseuille's constant of viscous flow ($m^3 \text{ s}^{-1} \text{ Pa}^{-1}$) (see context)
c_i	concentration (mol m^{-3})
c_p	specific heat at constant pressure ($J \text{ kg}^{-1} \text{ K}^{-1}$)
D	diffusion coefficient ($m^2 \text{ s}^{-1}$)
D^T	coefficient of thermal diffusion ($m^2 \text{ K}^{-1} \text{ s}^{-1}$)
D^D	Dufour coefficient ($m^2 \text{ K}^{-1} \text{ s}^{-1}$)
D_{12}	diffusion coefficient ($m^2 \text{ s}^{-1}$)
D^D	Dufour coefficient ($m^2 \text{ K}^{-1} \text{ s}^{-1}$)
D^T	coefficient of thermal diffusion ($m^2 \text{ K}^{-1} \text{ s}^{-1}$)
d	diameter of capillary (m)
E	electrode potential (V)
e'	ratio of bellows to tube volume, V/V (dimensionless)
f	compression factor for the middle tube when effect is maximized (dimensionless)
G	Gibbs free energy (J)
$G(T)$	function related to mass circulation rate (see Eq. 115)
g	acceleration due to gravity ($m \text{ s}^{-2}$)
$g(t)$	time function defined in Eq. (52) (dimensionless)
H	enthalpy (J) (see context)
\bar{H}	initial transport coefficient (kg s^{-1}) (see context)
\bar{H}_i	partial molar enthalpy of component i ($J \text{ mol}^{-1}$)
H_j	defined by Eq. (14) ($J \text{ mol}^{-1}$)
J	flux of matter ($\text{mol m}^{-2} \text{ s}^{-1}$ or $\text{kg m}^{-2} \text{ s}^{-1}$) (see context)

J_q	flux of heat ($J m^{-2} s^{-1}$)
J_s	flux of entropy ($J K^{-1} m^{-2} s^{-1}$)
K	molar composition at time t (dimensionless)
K	constant defined by Eq. (128)
K_0	convective remixing coefficient ($kg m s^{-1}$)
K_d	diffusive remixing coefficient ($kg m s^{-1}$)
K_z	spatial derivative of K (m^{-1})
k_T	thermal diffusion ratio (dimensionless)
k_B	Boltzmann constant ($J K^{-1}$)
L	length of connecting tube (m)
L_{ij}	phenomenological coefficient
l	length of capillary (m)
M	molar mass ($kg mol^{-1}$)
m	molality ($mol kg^{-1}$)
N	number of half-lives (dimensionless)
N_L	total molecular density in the connecting tube ($mol m^{-3}$)
n	refractive index (dimensionless) (see context)
n	total number of tubes (dimensionless) (see context)
n_1	number density ($mol m^{-3}$)
n_h	hydration number (dimensionless)
n_L	number density of the lighter component in the connecting tube ($mol m^{-3}$)
P	pressure (Pa)
P_0	initial or equilibrium pressure (Pa)
p	pressure (Pa)
Q	radial heat flow (Js^{-1}) (see context)
Q	overall separation factor (dimensionless) (see context)
Q^*	heat (enthalpy) of transport ($J mol^{-1}$)
q	elementary separation factor (dimensionless)
q_v	heat content per unit volume ($J m^{-3}$)
R	resistance (ohm)
R	gas constant ($J K^{-1} mol^{-1}$)
R^*	Stokes law radius (m)
r	radial coordinate (m)
r_c	radius of hot wall (m)
S	entropy ($J K^{-1}$)

S_V	entropy per unit volume ($J m^{-3} K^{-1}$)
S^*	entropy of transport ($J mol^{-1} K^{-1}$)
s	fraction of total tube length in each isothermal zone (dimensionless)
T	temperature (K)
T_0	initial gas temperature (K)
T_C	cold wall temperature (K)
T_H	hot wall temperature (K)
t_p	time for a complete pump cycle (s)
t	time (s) (see context)
t	Celsius temperature ($^{\circ}C$) (see context)
V	gas volume per tube (m^3) (see context)
V	volume (m^3) (see context)
\bar{V}	molar volume ($m^3 mol^{-1}$)
V_C	volume of cold bulb (m^3)
V_H	volume of hot bulb (m^3)
V_T	volume of connecting tube (m^3)
v_i	velocity ($m s^{-1}$)
\bar{v}	stream velocity ($m s^{-1}$)
W_i	Washburn number (dimensionless)
w_i	mass fraction of component i (dimensionless)
X	thermodynamic driving force
x_C	mole fraction of light component in cold bulb (dimensionless)
x_F	mole fraction of light component in feed mixture (dimensionless)
x_H	mole fraction of light component in hot bulb (dimensionless)
x_i	mole fraction of component i (dimensionless)
x_L	mole fraction of light component in connecting tube (dimensionless)
Y	resistance function defined by Eq. (61) (dimensionless)
Z_i	ionic valence (dimensionless)
z	linear variable (m)
α_T	thermal diffusion factor (dimensionless)
$\bar{\alpha}_T$	"effective" or average thermal diffusion factor (dimensionless)
β	defined by Eq. (65)
γ	column transport
Δx	change in mole fraction per unit area (m^{-2})
δ	correction factor for approach to equilibrium (dimensionless)

δT_a	temperature independent "diffusion thermoeffect", defined by Eq. (129) (K)
δT_b	temperature dependent "real" effect, defined by Eq. (130) (K)
ε	thermoelectric power ($V K^{-1}$) (see context)
ε	dielectric constant ($F m^{-1}$) (see context)
ε	correction factor for back diffusion in the capillaries (dimensionless) (see context)
ζ	correction factor for disturbance due to pumping (dimensionless)
η_T	viscosity of gas at operating temperature ($N s m^{-2}$)
Θ	relaxation time (s)
κ	thermal conductivity ($W m^{-1} K^{-1}$)
λ_i	ionic conductivity ($S m^2 mol^{-1}$)
Λ	molar conductivity ($S m^2 mol^{-1}$)
μ_i	chemical potential ($J mol^{-1}$)
μ_i	electrochemical potential ($J mol^{-1}$)
ν_i	amount of substance (mol)
ρ	density ($kg m^{-3}$)
σ	Soret coefficient (K^{-1})
τ	thermal relaxation time (s)
Φ	entropy source term ($J s^{-1} K^{-1}$)
ϕ	volume fraction (dimensionless)
ω	pumping frequency (s^{-1})

REFERENCES

- [1] C. Soret, Arch. Sci. Phys. Nat. Geneve., 2, 48 (1879); 4, 209 (1880) and Ann. Chim. Phys., 22, 293 (1881).
- [2] L. Dufour, Poggend. Ann. Physik, 148, 490 (1873).
- [3] J.R. deGroot, and P. Mazur, "Non-Equilibrium Thermodynamics" (Interscience, New York, 1962).
- [4] K.G. Denbigh, "The Thermodynamics of the Steady State" (Methuen, London, 1951).
- [5] D. Fitts, "Nonequilibrium Thermodynamics" (McGraw-Hill, New York, 1962).
- [6] A. Katchalsky, and P.F. Curran, "Nonequilibrium Thermodynamics in Biophysics", (Harvard University Press, Cambridge, 1965).
- [7] J.N. Agar, and J. Lin, J. Solution Chem., 16, 973 (1987).
- [8] J.N. Agar, C.Y. Mou, and J. Lin, J. Phys. Chemistry, to appear.
- [9] J.N. Agar, and J.C.R. Turner, Proc. Royal Soc., A255, 307 (1960).
- [10] D.G. Miller, J. Phys. Chem., 70, 2639 (1966).
- [11] H.J.V. Tyrrell, "Diffusion and Heat Flow in Liquids" (Butterworths, London, 1961).
- [12] J.A. Bierlein, J. Chem. Phys., 23, 10 (1955).
- [13] J.N. Agar, Trans. Faraday Soc., 56, 776 (1960).
- [14] F.H. Horne, and T.G. Anderson, J. Chem. Phys., 53, 2321 (1970).
- [15] J. Lin, J.A. Bierlein, and J.G. Becsey, J. Solution Chem., 3, 827 (1974).
- [16] J.N. Agar, and W.G. Breck, Trans. Faraday soc., 53, 167, 179 (1957).
- [17] J.N. Agar, (a) "Thermogalvanic Cells" Chapter 2 in Advances in Electrochemistry and Chemical Engineering, 1963, Volume 3, page 31; (b) Chapter 13 in "The Structure of Electrolyte Solutions", W.J. Hamer, ed., (Wiley, New York 1959).
- [18] C.J. Petit, M.H. Hwang, and J. Lin, J. Solution Chem., 17, 1 (1988).
- [19] G.J. Thomaes, J. Chim. Phys. 1956, 53, 407.
- [20] B.D. Butler, and J.C.R. Turner, Trans. Faraday Soc., 62, 3114, 3121 (1960).
- [21] M.H. Hwang, D. Robinson, E.J. Billo, and J. Lin, J. Solution Chem., 17, 83 (1988).
- [22] J.G. Becsey, J.A. Bierlein, and S.E. Gustafsoon, Z. Naturforschg., 219, 488 (1966).
- [23] S.E. Gustafsson, J.G. Becsey, and J.A. Bierlein, J. Phys. Chem., 69, 1016 (1965).
- [24] R.P. Rastogi and G.L. Madan, J. Chem. Phys., 48, 2372 (1965).
- [25] R.P. Rastogi, and B. L.S. Yadava, J. Chem. Phys., 51, 2826 (1969); 52, 2791 (1970).
- [26] S.E. Ingle, and F.H. Horne, J. Chem. Phys., 59, 5882 (1973).
- [27] R.L. Rowley, and F.H. Horne, J. Chem. Phys., 72, 131 (1980).
- [28] G. Platt, T. Vongvanich, and R.L. Rowley, J. Chem. Phys., 77, 2113 (1982).

- [29] G. Platt, T. Vongvanich, G. Fowler, and R.L. Rowley, *J. Chem. Phys.*, **77**, 2121 (1982).
- [30] H.K. Yow, B.P. Chakraborty, and J. Lin, *Electrochimica Acta*, **22**, 1013 (1977).
- [31] C.J. Petit, K. Renner, and J. Lin, *J. Solution Chem.*, **13**, 419 (1984).
- [32] C.J. Petit, M.H. Hwang, and J. Lin, *J. Solution Chem.*, **17**, 1 (1988).
- [33] C.J. Petit, M.H. Hwang, and J. Lin, *Int. J. Thermophysics*, **7**, 687 (1986).
- [34] H.S. Yow, and J. Lin, *J. Solution Chem.*, **12**, 487 (1983).
- [35] T.S. Thacher, C.Y. Mou, Y. Mobanty, and J. Lin, *J. Chem. Phys.*, **84**, 6401 (1986) and references cited.
- [36] M.H. Hwang, Ph.D. Thesis, Boston College, 1989.
- [37] N. Takeyama, and K. Nakashima, *J. Phys. Soc. Jpn.*, **52**, 2692, 2699 (1983); *J. Solution Chem.*, **17**, 305 (1988).
- [38] J. Lin, *J. Solution Chem.*, **8**, 125 (1979).
- [39] See for example "Electrolyte Solutions" by R.A. Robinson and R.H. Stokes, second ed. (Butterworths, London, 1959).
- [40] H.S. Frank, and E.W. Evans, *J. Chem. Phys.*, **13**, 507 (1945).
- [41] B.P. Chakraborty, and J. Lin, *J. Solution Chem.*, **5**, 183 (1976).
- [42] C.D. Wood, and W.A. Hawksworth, *J. South African Chem. Inst.*, **24**, 170 (1971).
- [43] H.J.V. Tyrrell, *Chem. Comm.*, 456 (1967).
- [44] P.S. Belton, and H.J.V. Tyrrell, *Z. Naturforsch. A*, **26**, 48 (1971).
- [45] G. Farsang, and H.J.V. Tyrrell, *J. Chem. Soc. A*, 1839 (1969).
- [46] T.G. Anderson, and F.H. Horne, *J. Chem. Phys.*, **55**, 2831 (1971).
- [47] M.J. Story, and J.C.R. Turner, *Trans. Faraday Soc.*, **65**, 1523 (1969).
- [48] J.C. Johnson, and A.L. Beyerlein, *J. Phys. Chem.*, **182**, 1430 (1978).
- [49] N-Y. R. Ma, and A.L. Beyerlein, *J. Phys. Chem.*, **87**, 245 (1983).
- [50] N-Y. R. Ma, D. Stanford, and A.L. Beyerlein, *J. Phys. Chem.*, **87**, 5464 (1983).
- [51] N-Y. R. Ma, and A.L. Beyerlein, *J. Chem. Phys.*, **78**, 7010 (1983).
- [52] W. M. Rutherford, *J. Chem. Phys.*, **81**, 6136 (1984).
- [53] W. M. Rutherford, *J. Chem. Phys.*, **86**, 397 (1987).
- [54] W. M. Rutherford, *J. Chem. Phys.*, **86**, 5217 (1987).
- [55] C.J. Petit, J. Lin, and K. Renner, *J. Phys. Chem.*, **88**, 2435 (1984); **78**, 7010 (1983).
- [56] J.B. Baranowski, A.E. deVries, A. Haring, and R. Paul, *Adv. Chem. Phys.*, **16**, 101 (1969).
- [57] J.A. Barker, and F. Smith, *J. Chem. Phys.*, **22**, 375 (1954).
- [58] C. Wagner, *Ann. der Physik(V)*, **3**, 629 (1929).
- [59] R.L. Rowley, and M.D. Hall, *J. Chem. Phys.*, **85**, 3550 (1986).

- [60] S.C. Yi, and R.L. Rowley, *J. Chem. Phys.*, **87**, 7208 (1987).
- [61] S.C. Yi, and R.L. Rowley, *J. Chem. Phys.*, **87**, 7214 (1987).
- [62] R.J. Bearman, J.G. Kirkwood, and M. Fixman, *Adv. Chem. Phys.*, **1**, 1 (1958).
- [63] A.G. Guy, *Int. J. Thermophys.*, **7**, 563 (1986).
- [64] R.G. Mortimer, and H. Eyring, *Proc. Natl. Acad. Sci. U.S.A.*, **77**, 4 (1980).
- [65] L. Barajas, L.S. Garcia-Colin, and E. Pina, *J. Stat. Phys.*, **7**, 161 (1973).
- [66] I.L. McLaughlin, and T. Davis, *J. Chem. Phys.*, **45**, 6 (1966).
- [67] D. Enskog, *Phys. Z.* **12**, 56 (1911); *ibid.*, 533 (1911).
- [68] D. Enskog, Inaugural Dissertation, University of Uppsala (Sweden), 1917.
- [69] S. Chapman, *Philos. Trans. A* **217**, 115 (1917).
- [70] S. Chapman and F. W. Dootson, *Phil. Mag.* **33**, 248 (1917).
- [71] E. A. Mason, *J. Chem. Phys.* **27**, 75 (1957).
- [72] T. L. Ibbs, *Proc. Roy. Soc. A* **107**, 470 (1925).
- [73] W. L. Taylor, D. Cain, F. R. Meeks, and P. T. Pickett, *J. Chem. Phys.* **82**, 2745 (1985).
- [74] H. K. Lonsdale and E. A. Mason, *J. Phys. Chem.* **61**, 1544 (1957).
- [75] A. I. Ghozlan and J. Los, *J. Chem. Phys.* **60**, 178 (1960).
- [76] S. Weissman, *Phys. Fluids* **12**, 2337 (1967).
- [77] W. L. Taylor, *J. Chem. Phys.* **88**, 7097 (1988).
- [78] H. K. Lonsdale and E. A. Mason, University of Maryland Rept. IMP-AEC-2, Pt. II, Appendix A, p. 119 (1957).
- [79] K. E. Grew and A. E. Humphreys, *J. Chem. Phys.* **45**, 4267 (1966).
- [80] C. A. Velds, J. Los, and A. E. de Vries, *Physica* **35**, 417 (1967).
- [81] J. M. Symons, M. L. Martin, and P. J. Dunlop, *J. Chem. Soc. Faraday I* **75**, 621 (1979).
- [82] R. D. Trengrove, H. L. Robjohns, T. N. Bell, M. L. Martin, and P. J. Dunlop, *Physica A* **108**, 488 (1981).
- [83] K. Clusius and M. Huber, *Z. Naturforsch.* **10a**, 230 (1955).
- [84] B. L. van der Waerden, *Z. Naturforsch.* **12a**, 583 (1957).
- [85] W. L. Taylor, S. Weissman, W. J. Haubach, and P. T. Pickett, *J. Chem. Phys.* **50**, 4886 (1969).
- [86] W. L. Taylor, D. Cain, F. R. Meeks and P. T. Pickett, *J. Chem. Phys.* **82**, 2745 (1985).
- [87] T. I. Moran and W. W. Watson, *Phys. Rev.* **109**, 1184 (1958).
- [88] W. W. Watson, A. J. Howard, N. E. Miller, and R. M. Shiffrin, *Z. Naturforsch.* **18a**, 242 (1963).
- [89] R. Paul, A. J. Howard, and W. W. Watson, *J. Chem. Phys.* **39**, 3053 (1963); *ibid* **43**, 1890 (1965).
- [90] M. F. Laranjeira and J. Kistemaker, *Physica* **26**, 431 (1960).

-
- [91] M. F. Laranjeira, Thesis, Leiden (1959).
- [92] F. van der Valk, Thesis, Amsterdam (1963).
- [93] F. van der Valk and A. E. de Vries, *Physica* **29**, 427 (1963).
- [94] M. F. Laranjeira and M. A. Cunha, *Port. Phys.* **4**, 281 (1966).
- [95] W. A. Oost and A. Haring, *Z. Naturforsch.* **25a**, 1879 (1970).
- [96] K. Clusius and G. Dickel, *Naturwiss.* **26**, 546 (1938).
- [97] W. H. Furry, R. Clark Jones, and L. Onsager, *Phys. Rev.* **55**, 1083 (1939).
- [98] W. H. Furry and R. Clark Jones, *Phys. Rev.* **69**, 459 (1946).
- [99] R. Clark Jones and W. H. Furry, *Rev. Mod. Phys.* **18**, 151 (1946).
- [100] W. M. Rutherford, *J. Chem. Phys.* **53**, 4319 (1970).
- [101] Von J. Schirdewahn, A. Klemm, and L. Waldmann, *Z. Naturforsch.* **16a**, 133 (1961).
- [102] A. E. de Vries and A. Haring, *Z. Naturforsch.* **19a**, 225 (1964).
- [103] S. Raman, S. M. Dave, and T. K. S. Narayanan, *Phys. Fluids* **8**, 1964 (1965).
- [104] S. Raman, R. Paul and W. W. Watson, *J. Chem. Phys.* **46**, 3916 (1967).
- [105] P. Kirch and R. Schütte, *J. Chem. Phys.* **42**, 3729 (1965).
- [106] J. M. Savirón, C. M. Santamaría, J. A. Carrión and J. C. Yarza, *J. Chem. Phys.* **63**, 5318 (1975).
- [107] C. M. Santamaría, J. M. Savirón, J. C. Yarza and J. A. Carrión, *J. Chem. Phys.* **64**, 1095 (1976).
- [108] C. M. Santamaría, J. M. Savirón, J. C. Yarza and J. A. Carrión, *Physica* **82A**, 90 (1977).
- [109] W. M. Rutherford, *J. Chem. Phys.* **54**, 4542 (1971).
- [110] W. M. Rutherford and K. J. Kaminski, *J. Chem. Phys.* **47**, 5427 (1967).
- [111] L. Waldmann, *Z. Naturforsch.* **4a**, 105 (1949).